

863462

**DISCRETE SLIDING MODE CONTROL USING IN
A SCARA ROBOT BY DIGITAL COMPUTER**

By

WEI-GUANG CHEN

Bachelor of Science

Chung-Yuan Christian University

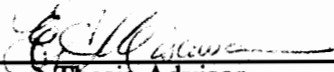
Chung-Li, Taiwan

1987

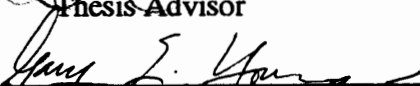
**Submitted to the Faculty of the
Graduate College of the
Oklahoma State University
in partial fulfillment of
the requirements for
the Degree of
MASTER OF SCIENCE
May, 1993**

DISCRETE SLIDING MODE CONTROL USING IN
A SCARA ROBOT BY DIGITAL COMPUTER


Thesis Approved:



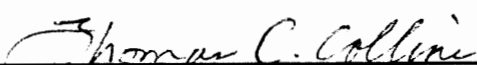
Thesis Advisor



Guy L. Young



J. P. McLaughlin



Thomas C. Collins
Dean of Graduate College

ACKNOWLEDGMENTS

The author would like to express his sincere appreciation and thanks to many people who encourage his graduate program.

A special note of appreciation is extended to the principal advisor, Dr. E. A. Misawa, for his guidance, patience, and encouragement throughout the graduate program.

Many thanks Also go to Dr. G. E. Young and Dr. L. L. Hoberock for serving the graduate committee. From their advises and suggestions, I obtain many valuable experiences to this study.

My sincerest appreciation is expressed to my parents and other family members, without their support, understanding, and encouragement this undertaking would have been impossible.

Most of all, I thank God for his kindness and love beside me all through my life.

TABLE OF CONTENTS

Chapter	Page
I. INTRODUCTION	1
II. PREVIEW INVESTIGATION	4
Introduction	4
Continuous Sliding Mode Control	4
Chattering	10
Discrete Sliding Mode Control	17
III. METHODOLOGY AND MODEL	25
Introduction	25
Continuous Time Controller Design	25
Stability Analysis	26
Discrete Time Controller Design	27
Square Method	28
Discrete Time Sliding Mode Control Law	29
Stability Analysis	31
Reaching Phase	32
Inside the Boundary Layer	32
Model Description	33
Introduction	34
Two-Link Robot Model	34
IV. SIMULATIONS AND RESULTS	39
Application to a SCARA Robot	39
Implementation of Discrete Time Sliding Mode Control	40
Uncertain System	40
Stability Analysis	43
Reaching Phase	43
Inside the Boundary Layer	43

Chapter	Page
Simulation Discussions	47
Effect of Sampling Time47
Effect of Boundary Layer Thickness48
Trade off Between Reaching Rate and Sampling Time	49
V. CONCLUSIONS AND RECOMMENDATIONS	78
Conclusions78
Recommendations79
BIBLIOGRAPHY	81
APPENDIX - MODEL DESCRIPTION OF THE SCARA ROBOT AND DYNAMIC EQUATION DERIVED84

LIST OF FIGURES

Figure	Page
1. Sliding Mode in the Intersection of Discontinuity Surface.	7
2. Graphical Interpretation of Sliding Mode Control.	9
3. Filippov's Construction of the Equivalent Dynamics.	12
4. Chattering as a Result of Switching Control.	13
5. The Boundary Layer.	15
6. Control Behavior in the Boundary Layer.	16
7. The Approaching Behavior of Discrete Sliding Mode.	18
8. Model of the Sliding Line Control.	21
9. Model of the Sliding Trajectory Control.	22
10. The Model of SCARA Robot.	35
11. Model Checking Simulation.	38
12. The Root Locus of Discrete Time Sliding Mode Control for SCARA Robot with $\beta = 1$	46
13. 1-st Link Trajectory and Desired Trajectory $\lambda = 5 \quad \Delta t = 0.01 \quad \Phi = 0.02 \quad \gamma = 0.01$	50
14. 2-nd Link Trajectory and Desired Trajectory $\lambda = 5 \quad \Delta t = 0.01 \quad \Phi = 0.02 \quad \gamma = 0.01$	51
15. $s_1(k)$ $\lambda = 5 \quad \Delta t = 0.01 \quad \Phi = 0.02 \quad \gamma = 0.01$	52
16. $s_2(k)$ $\lambda = 5 \quad \Delta t = 0.01 \quad \Phi = 0.02 \quad \gamma = 0.01$	53
17. Zooming of $s_1(k)$ $\lambda = 5 \quad \Delta t = 0.01 \quad \Phi = 0.02 \quad \gamma = 0.01$	54

Figure	Page
18. Zooming of $s_2(k)$ $\lambda = 5 \quad \Delta t = 0.01 \quad \Phi = 0.02 \quad \gamma = 0.01$	55
19. 1-st Link Trajectory and Desired Trajectory $\lambda = 5 \quad \Delta t = 0.05 \quad \Phi = 0.02 \quad \gamma = 0.01$	56
20. 2-nd Link Trajectory and Desired Trajectory $\lambda = 5 \quad \Delta t = 0.05 \quad \Phi = 0.02 \quad \gamma = 0.01$	57
21. $s_1(k)$ $\lambda = 5 \quad \Delta t = 0.05 \quad \Phi = 0.02 \quad \gamma = 0.01$	58
22. $s_2(k)$ $\lambda = 5 \quad \Delta t = 0.05 \quad \Phi = 0.02 \quad \gamma = 0.01$	59
23. Zooming of $s_1(k)$ $\lambda = 5 \quad \Delta t = 0.05 \quad \Phi = 0.02 \quad \gamma = 0.01$	60
24. Zooming of $s_2(k)$ $\lambda = 5 \quad \Delta t = 0.05 \quad \Phi = 0.02 \quad \gamma = 0.01$	61
25. 1-st Link Trajectory and Desired Trajectory $\lambda = 5 \quad \Delta t = 0.2 \quad \Phi = 0.02 \quad \gamma = 0.01$	62
26. 2-nd Link Trajectory and Desired Trajectory $\lambda = 5 \quad \Delta t = 0.2 \quad \Phi = 0.02 \quad \gamma = 0.01$	63
27. $s_1(k)$ $\lambda = 5 \quad \Delta t = 0.2 \quad \Phi = 0.02 \quad \gamma = 0.01$	64
28. $s_2(k)$ $\lambda = 5 \quad \Delta t = 0.2 \quad \Phi = 0.02 \quad \gamma = 0.01$	65
29. 1-st Link Trajectory and Desired Trajectory $\lambda = 10 \quad \Delta t = 0.05 \quad \Phi = 0.05 \quad \gamma = 0.025$	66
30. 2-nd Link Trajectory and Desired Trajectory $\lambda = 10 \quad \Delta t = 0.05 \quad \Phi = 0.05 \quad \gamma = 0.025$	67
31. $s_1(k)$ $\lambda = 10 \quad \Delta t = 0.05 \quad \Phi = 0.05 \quad \gamma = 0.025$	68
32. $s_2(k)$ $\lambda = 10 \quad \Delta t = 0.05 \quad \Phi = 0.05 \quad \gamma = 0.025$	69
33. Zooming of $s_1(k)$ $\lambda = 10 \quad \Delta t = 0.05 \quad \Phi = 0.05 \quad \gamma = 0.025$	70
34. Zooming of $s_2(k)$ $\lambda = 10 \quad \Delta t = 0.05 \quad \Phi = 0.05 \quad \gamma = 0.025$	71

Figure	page
35. 1-st Link Trajectory and Desired Trajectory $\lambda = 50 \quad \Delta t = 0.02 \quad \Phi = 0.05 \quad \gamma = 0.025$	72
36. 2-nd Link Trajectory and Desired Trajectory $\lambda = 50 \quad \Delta t = 0.02 \quad \Phi = 0.05 \quad \gamma = 0.025$	73
37. $s_1(k)$ $\lambda = 50 \quad \Delta t = 0.02 \quad \Phi = 0.05 \quad \gamma = 0.025$	74
38. $s_2(k)$ $\lambda = 50 \quad \Delta t = 0.02 \quad \Phi = 0.05 \quad \gamma = 0.025$	75
39. Zooming of $s_1(k)$ $\lambda = 50 \quad \Delta t = 0.02 \quad \Phi = 0.05 \quad \gamma = 0.025$	76
40. Zooming of $s_2(k)$ $\lambda = 50 \quad \Delta t = 0.02 \quad \Phi = 0.05 \quad \gamma = 0.025$	77

NOMENCLATURE

C	Sliding Mode Constant Vector
d	Disturbance and Uncertainty Vector
g	Gravity Acceleration
H	Modeling error and Disturbances Matrix
j1	Total Moment of Inertia of 1st link
j2	Total Moment of Inertia of 2nd link
J	Inertia Matrix
K	Kinetic Energy
L	Mechanical Energy
L1	Length of 1st link
L2	Length of 2nd link
l1	Distance of 1st link Center of Mass to Joint O
l2	Distance of 2nd link Center of Mass to Joint A
m1	Concentrate-mass of 1st link
m2	Concentrate-mass of 2nd link
S	Sliding Surface
η	Switching Positive Constant
V	Potential Energy
Φ	Boundary Layer Thickness
ε	Boundary Layer Width

- Γ Applied Torque
- Δt Sampling Time
- λ Reaching Rate
- θ_1 Angular Displacement of 1st link about to Vertical Line
- θ_2 Angular Displacement of 2nd link about 1st Link

CHAPTER I

INTRODUCTION

Robotics manipulators used in industry to do repetitive jobs are important course in engineering area to mass-produce high-quality properties. High performance is required, that is, high speed, high precision, convenience and durability are expected from modern industrial robots.

Sliding mode control is one of the robust control design techniques. Especially when modeling inaccuracies occur in the system, sliding mode control shows its merits in maintaining stability and consistent performance in both linear and nonlinear systems.

The sliding mode control is basically an adaptive control method where the response is forced to track or 'slide' along a predefined trajectory. Sliding mode control is composed of a nominal part, similar to a feedback linearization, and of an additional part which deal with system uncertainties. It has been successfully used in robot manipulators, transmissions and engines of automobiles, electronic motors etc..

The flexibility and low cost of digital computers motivated the use of digital control in a variety of products. However, the sliding mode control algorithms is mostly discussed by engineers in analogous domain. Some engineers obtained good results by implementing the analog algorithms to digital computers. Most designers usually depend on their individual expertise and experiences in the choice of sampling time. None of them had ever

talked about the determination of a sampling period and its effect in the stability of the sliding mode control.

The sampling period plays an important role in the discrete time control. When a well-developed continuous time domain theory is used in a digital computer, we normally choose the sampling time as small as possible in order to let the controller behave like a continuous one. It is known that a sampling time that is not small enough will make a theoretically stable control system unstable.

When the sliding mode controller is sampled at each sampling time, the system behaves as a sliding mode control. Between sampling interval, the control input remains at the same value until the next sampling. During the sampling interval, inevitably, a nonideal sliding regime will appear. This quasi-sliding regime is inherently different from the quasi-sliding regime which may appear in the continuous time system due to nonideal behavior of analog component [9] and may make the system unstable.

This research is dedicated to the design of the discrete time sliding mode control for a n -th order canonical form of a single input time variant nonlinear system with the derivation of control law and stability analysis. This paper implements the discrete time sliding mode control to a SCARA robot and discusses the stability affected by different parameters. People usually use a fast sampling time on controllers in order to make the system stable. In the mean time, the cost of the product will be higher correspondingly and sometimes it just wastes money to build up such a controller with a high sampling rate. Also, during the sampling period the dynamics of the system have not been discussed yet. Therefore, this research provides an easier and cheaper way to construct a discrete time sliding mode control in the use of digital computer.

The next chapter, chapter 2, investigates the sliding mode control used in industry. There are people successfully using it in many systems in both continuous and discrete time domain.

Chapter 3 introduces the square method that deals with the discrete time sliding mode control used in a single input time variant nonlinear system in n-th order canonical form. A stability analysis discussion is also presented. Moreover, we introduce the SCARA robot's dynamic equation which is a 2nd-order nonlinear differential equation.

Chapter 4 shows the implementation of discrete time sliding mode control to the SCARA robot with numerical values applied to it. This chapter also presents a crucial result of an investigation of the effect of the sampling time on the stability. The simulations of the control algorithm are also demonstrated in this chapter. Chapter 5 presents the conclusions of this paper and recommendations about future works.

CHAPTER II

PREVIEW INVESTIGATION

Introduction

New industrial robotics need quick controller design and less tracking errors in order to reach desired fast motion. Researchers use various methods to build up controller in dealing with linear and nonlinear systems. Sliding mode control provides an adequate way to maintain stability and consistent performance in the face of modeling imprecision [24]. Sliding mode control, also known as variable structure control system, has been developed over twenty-five years in the world. Although the sliding mode control theory is well developed, there are some obstacles in practical application. Especially in the use of digital computer the discrete time sliding mode control is not yet discussed. This chapter reviews previous researches regarding sliding mode control and its implementation.

Continuous Sliding Mode Controller

Sliding mode control is a control algorithm which initially defines a sliding surface by using tracking errors and then regulates the system to the desired point. Basically, sliding mode control is an adaptive control method where the response is forced to slide along a predefined surface, sliding surface. In order to increase the robustness of the close loop system, sliding mode controller implements switching action in the feedback loop. In the ideal case, sliding mode control is insensitive to the plant parameter uncertainties and external disturbances [33]. The sliding mode control is actually one of the algorithms that can guarantee (at least theoretically) whole system robustness for various plants and disturbance [1], and many people prefer to use it.

Previous researches examine sliding mode control. In the works of Klein and Maney [15], Erschler and co-workers [9], variable structure control, which is another form of sliding control, has been proven to be, from the viewpoint of robustness, a useful tool in plants even though the parameter's uncertainties occur. Emilyanov [8] used it in 1967 as application and Utkin [30] discusses in detail the changing structures according to the switching logic.

However, some non-idealities associated with the implementation will generate 'chattering' in the switching surface, sliding surface, which will cause an undesirable high-frequency component in the state trajectories. Slotine and Sastry [26] show a methodology of approximate continuous control law that makes sliding mode control more robust. Especially in the neglecting of high-frequency dynamics, which are unmodeling dynamics in the system, the piecewise continuous feedback control law could avoid touching it.

We will consider the following system to present the main idea of sliding mode control.

$$\ddot{x} + a\dot{x} + d(t,x) = u \tag{1}$$

where $x \in \mathbb{R}^n$ is the state variable

$u \in \mathbb{R}^m$ is control input

$d \in \mathbb{R}^n$ is uncertainty vector

The uncertainty vector is assumed bounded.

Define: A set of discontinuity surface, sliding surface, to be S_i in state space as shown in Figure 1.

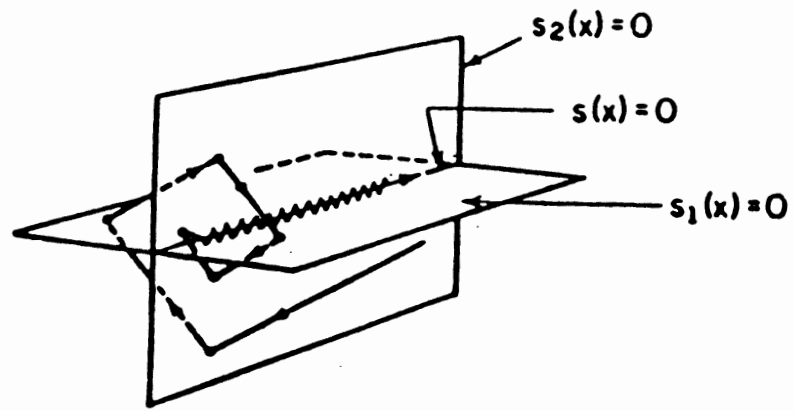


Figure 1. Sliding Mode in the Intersection of Discontinuity Surface

$$S_i = c_i^T x \quad i=1,2,3,\dots,m$$

where $c_i \in R^m$ is a constant vector

The control law must be designed under this constraint in order to keep the system's states on the neighborhood of the sliding surface. So the system will show sliding mode and become insensitive to parameter uncertainty and input disturbance. The system in sliding mode control should behave like Figure 2.

The sliding condition along the sliding surface is

$$\frac{d}{dt} \left(\frac{1}{2} S_i^2(x,t) \right) < 0 \quad \text{for } i=1,2,3,\dots,m$$

This is evaluated along the trajectory of sliding surface.

For the global sliding condition is

$$\frac{d}{dt} (S_i^2(x,t)) \leq -\eta |S|$$

where η is switching positive constant

Essentially, the distance square to the surface, measured by S^2 , decrease all system trajectories. Also, if $x(t=0) \neq x_d(t=0)$, the surface $S(t)$ will nevertheless be reached in a finite time.

We can integrate the equation and get

$$\int_0^t \frac{d}{dt} S^2 \leq \int_0^t -\eta |S|$$

$$\int_0^t d |S| \leq \int_0^t -\eta dt$$

$$S(t) - S(0) = 0 - S(0) \leq -\eta (t_{\text{reach}} - 0)$$

$$t_{\text{reach}} \leq |S(0)| / \eta$$

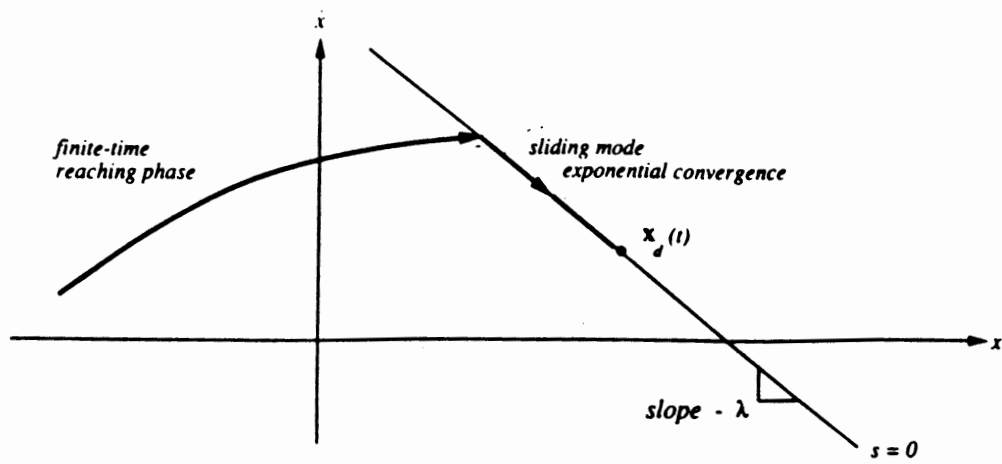


Figure 2. Graphical Interpretation of Sliding Mode Control

Chattering

The control law is determined by selecting a function of the tracking error s . Meanwhile, s^2 will present a Lyapunov-like function of the close loop system despite the existence of unmodeled dynamics and input disturbance.

$$\ddot{\tilde{x}} + a\dot{\tilde{x}} + d(t,x) = u$$

Define

$$s = \left(\frac{d}{dt} + \lambda \right)^{n-1} \tilde{x}$$

where

$$n=2$$

$$\tilde{x} = x - x_d$$

$$\dot{s} = \dot{\tilde{x}} + \lambda\tilde{x}$$

$$= \ddot{x} - \ddot{x}_d + \lambda\dot{\tilde{x}}$$

$$= u - a\dot{\tilde{x}} - d(t,x) - \ddot{x}_d + \lambda\dot{\tilde{x}} \leq -k^* \operatorname{sgn}(s)$$

If the disturbance $d(t,x)$ is bounded and all the parameter uncertainties are bounded, then we can find a lower bound of value k .

$$\dot{s} = u - a\dot{\tilde{x}} - \ddot{x}_d + \lambda\dot{\tilde{x}} \leq -k \operatorname{sgn}(s)$$

$$u \leq a\dot{\tilde{x}} + \ddot{x}_d - \lambda\dot{\tilde{x}} - k \operatorname{sgn}(s)$$

where

$$\operatorname{sgn}(s) = 1 \quad s > 0$$

$$= -1 \quad s < 0$$

The sign function will switch the control law according to the sign of s . A very famous example that Filippov shows is the construction of the equivalent dynamics in the sliding mode shown in Figure 3.

The discontinuity control law from the above equation will cause 'chattering' in Figure 4 when crossing the sliding surface $s(t)$.

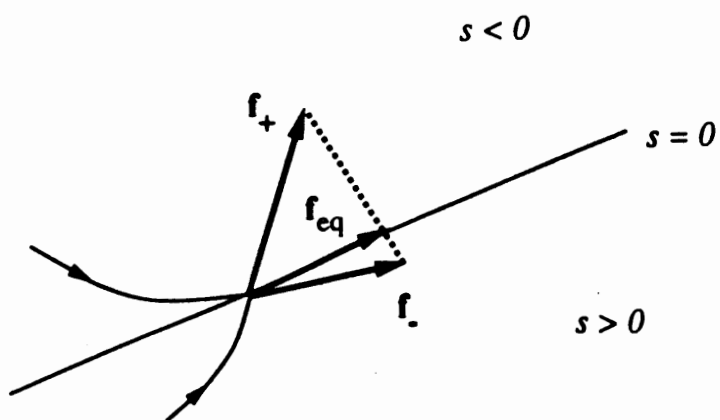


Figure 3. Filippov's Construction of the Equivalent Dynamics

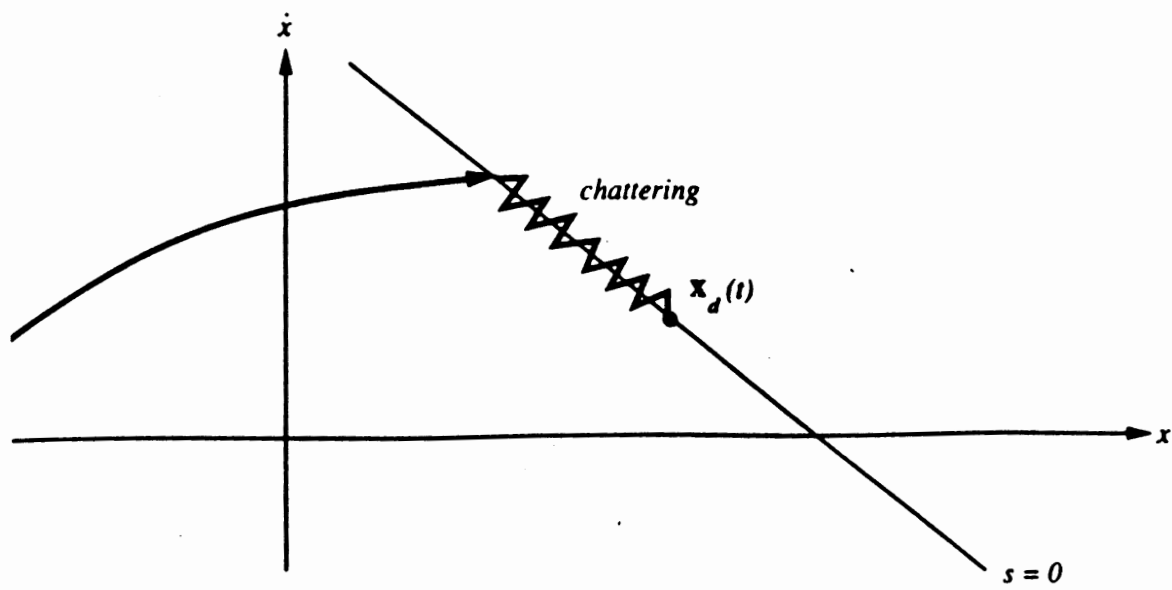


Figure 4. Chattering as a Result of Switching Control

Chattering is undesirable in the real implementation because it causes high control authority, and probably excites the high-frequency dynamics, such as modeling error, time delay, etc., which we neglected in the early assumption.

While this drawback stocks the sliding mode control to be used in the practical industry, its merit of good robustness can not be neglected. Some specific people still focus on the sliding mode control and revise their theories. Slotine and Sastry [26] define a thin boundary layer in the neighborhood of the switching surface, as shown in Figure 5, to smooth out the control discontinuity.

$$B(t) = \{ x \mid s(t,x) \leq \Phi \} \quad \Phi > 0$$

where Φ is the boundary layer thickness

and, also, boundary width ε is defined as

$$\varepsilon = \Phi / \lambda^{n-1}$$

This idea turns out to be that when the tracking error is outside boundary layer, the control law is still the same control input u , which means attracting to the sliding surface. After reaching the boundary layer, Slotine uses the piecewise continuous function, saturation function as shown in Figure 6, instead of the sign function, in order to smooth the chattering and present a decent result in the implementation of robotics arm manipulator.

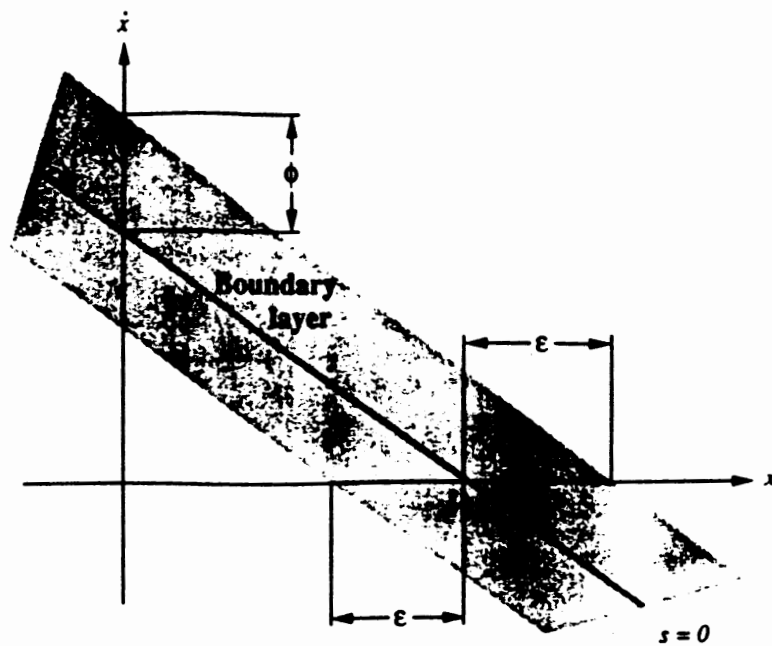


Figure 5. The Boundary Layer

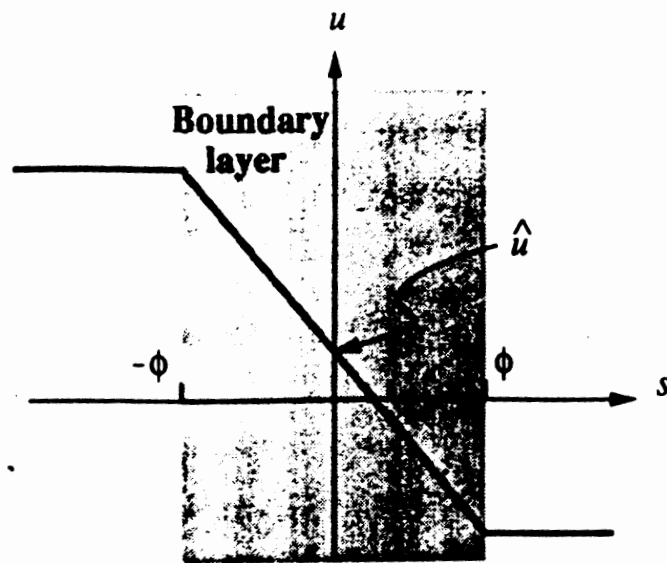


Figure 6. Control Behavior in the Boundary Layer

Discrete Time Controller

The digital computer has been widely used in many aspects; and the control of the physical system, through the digital control, has become increasingly common. However, those control algorithms we previously mentioned are discussed by engineers mostly in an analogous way. There have been some engineers utilizing them with digital computers and they have obtained some good results [3] [4] [5] [6] [10] [14] [17] [22] [28].

Milosavljevic [17] first proves the existence of the quasi-sliding mode on the switching hyperplane in the discrete time sliding mode control. With certain necessary conditions the trajectory can reach the sliding surface. However, he does not mention the behavior of the trajectory after the trajectory hits the discontinuous hyperplane. Drakunov and Utkin [6] have studied the definition of the discrete-time sliding mode control, and have discovered that the design of the discrete time sliding mode control algorithm has properties similar to those in continuous time systems with sliding mode control algorithms. It also shows the quasi-sliding in the discrete time sliding mode control that would be the behavior of the trajectory to reach the desired point as show in Figure 7. The behavior of the trajectory fluctuates and converges on the sliding surface, going to the desired point; it doesn't like the continuous sliding mode.

The practical application of the sliding mode control is widely used in different motor drive systems because of its robust properties. Some of the implementations are used in microprocessor based drives. Dote, Takebe and Ito [5] use an analog IC to implement the sliding mode control into a DC motor drive speed regulation. In addition to this, an algorithm obtained by rotating the sliding curve adaptively is extensively applied in order to achieve the sub-time optimal control. Dote and Hoft [4] use the sliding mode control algorithm in a microprocessor for DC motor drives. They use their own experimental value of the sampling time on simulations and on the microprocessor.

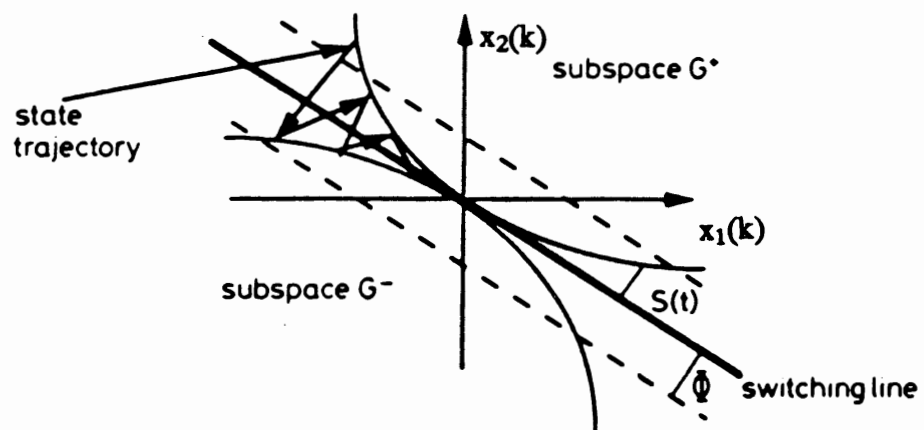


Figure 7. The Approaching Behavior of Discrete Sliding Mode

In another paper, Espana, Ortega and Espino [10] propose a method to allow the designer to simultaneously satisfy the conflicting requirements of the reaching time to the sliding plane and the transient behavior degradation due to the effect of the chattering. The proposed strategy considers the vicinity of the sliding surface like a boundary layer, in which the feedback gain is adjusted to obtain a state velocity vector almost parallel to it.

Sarpturk, Istefanopulos and Kaynak [22] propose an upper bound and a lower bound of control that can guarantee the stability of discrete-time sliding mode control. Spurgeon [28] investigated the paper of Sarpturk, Istefanopulos and Kaynak [22] which provided an upper bound and lower bound of the control input that can stabilize the systems. Spurgeon also verified that the discrete time sliding mode control strategy [22] can reduce the effect of external disturbances, but he did not guarantee attainment of the sliding mode. An alternative approach to a linear system he used was the linear feedback control structure. However, he has not proven that it is necessary to incorporate a discontinuous/ nonlinear feedback component in the application of the discrete VTOL (Generic Vertical Take-Off and Landing) aircraft system.

Bose [3] was the first one to simulate the induction motor drive system on a digital computer using SIMNON language; this was then experimentally verified in a laboratory both for sliding line and sliding trajectory control. The idea of sliding line control is shown in Figure 8. The initial point is located at point A and crosses the sliding line to point B. At point B the system is switched back to positive feedback mode and the trajectory will follow some specific curve to cross the line at point C. The sliding line control system will converge in this way. On the other hand, the model of the sliding trajectory control is shown in Figure 9. The sliding trajectory control is better than the sliding line control. The sliding line control has a disadvantage in the reaching phase and may drift due to the parameters variation and load disturbance effects. He divides the sliding trajectory control into three modes: acceleration region, constant speed region and the deceleration region.

This division into three region allows the sliding trajectory control to overcome the parameters variation and load disturbance.

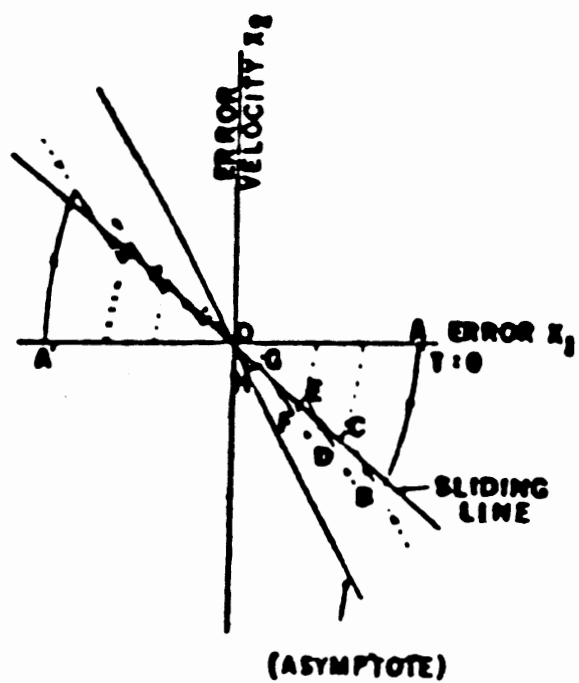


Figure 8. Model of the Sliding Line Control

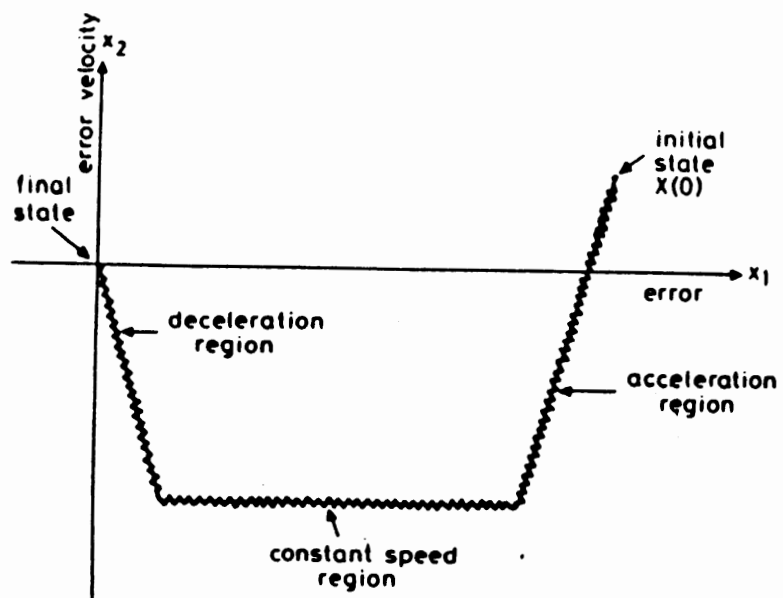


Figure 9. Model of the Sliding Trajectory Control

The work of Habibi and Richards [12] presents the combination of discrete time sliding mode control, computed torque technique, and use of this combination algorithm on an electrically powered industrial robot. Furthermore, the computed torque has been rectified by an additional input to improve the ability to tolerate parameter uncertainties.

Karunadasa and Renfrew [14] present a consideration of a practical sampling period used in a microprocessor based sliding mode controller for a brushless DC servomotor drive. They experimentally investigate the effects of the sampling time on the system performance and found the fine tune of each controller's parameter. But none of the previous studies had ever theoretically discussed about the determination of sampling time and the effective of the sampling time to the stability.

Slotine discusses the sliding mode control in the analog domain in [25], but he does not refer to the discrete time case. As engineers apply Slotine's technique to digital control, the determination of the sampling time becomes difficult.

This study is concerned with the discrete time sliding mode control algorithm designed for a n th-order time variant nonlinear system given in a canonical form. This research introduces square method in dealing with discrete time sliding mode control. In the mean time, for the system stability, this research check the effects of the sampling time. This paper will also show a technique to determine the sampling time based upon stability theory.

The sampling time plays an important role in the discrete time control, especially in the use of digital computer. It will make a stable control system unstable if the sampling time is not small enough. This paper illustrates an example on a 2nd-order nonlinear time variant system using discrete time sliding mode control.

This research also found that some other design parameters will affect the system's stability, as in the reaching rate and boundary layer thickness. To design a discrete time sliding mode controller, designer will have more restrictions than to design a continuous one.

In order to analyze robustness this study use a two-link robotics arm manipulator as a model, whose parameters are not only time-varying but also nonlinear. The robot model, discrete controller design, and robustness analysis will be discussed in the next chapter.

CHAPTER III

METHODOLOGY AND MODEL DESCRIPTION

Introduction

This chapter outlines the analysis of the discrete time sliding mode control by the way of Lyapunov equation. It illustrates a two link robot manipulator as an implementation.

Divided into two sections, this chapter contains:

- * Continuous-time controller design
- * Discrete-time controller design
 - * Discrete-time sliding mode control
 - * Stability analysis

Continuous Time Controller Design

A n-th order continuous nonlinear system in canonical form could be expressed as

$$\dot{x}_1 = x_2$$

$$\dot{x}_2 = x_3$$

$$\vdots$$

$$\dot{x}_n = f(x_1, x_2, \dots, x_n) + g(x_1, x_2, \dots, x_n) u$$

Define the sliding hyperplane s

$$s = C \tilde{x}$$

where

$$C = [c_1, c_2, \dots, c_n] \quad c_i \neq 0, \quad i = 1, 2, \dots, n$$

$$\tilde{x} = x - x_d$$

We differentiate the s with respect to time and get

$$\begin{aligned} \dot{s} &= C \dot{\tilde{x}} \\ &= c_1 \dot{x}_1 + c_2 \dot{x}_2 + \dots + c_n \dot{x}_n - (c_1 \dot{x}_{1d} + c_2 \dot{x}_{2d} + \dots + c_n \dot{x}_{nd}) \end{aligned} \quad (2)$$

Plugging in the system dynamics, the equation (2) will be

$$\begin{aligned} \dot{s} &= c_1 \dot{x}_1 + c_2 \dot{x}_2 + \dots + c_n f(x_1, x_2, \dots, x_n) + c_n g(x_1, x_2, \dots, x_n) u \\ &\quad - C \dot{x}_d < -k \text{sat}(s) \end{aligned}$$

where

k is the upper bound of the value of \dot{s}

$$\text{sat}(s) = \begin{cases} \frac{s}{|s|} = \text{sgn}(s) & \text{for } |s| \geq \Phi \\ \frac{s}{\Phi} & \text{for } |s| < \Phi \end{cases}$$

Φ is the boundary layer thickness

We can get the control law as

$$u = \frac{-(c_1 \dot{x}_1 + c_2 \dot{x}_2 + \dots + c_n f(x_1, x_2, \dots, x_n) - C \dot{x}_d + k \text{sat}(s))}{g(x_1, x_2, \dots, x_n)}$$

Stability Analysis

Plugging the control law into the system dynamics we get

$$\begin{aligned} \dot{\mathbf{x}}_n = & - (c_1 \dot{x}_1 + c_2 \dot{x}_2 + \dots + c_{n-1} \dot{x}_{n-1}) + (1 - c_n) f(x_1, x_2, \dots, x_n) \\ & + C \dot{x}_d - k \text{sat}(s) \end{aligned}$$

Normally, we choose $c_n = 1$

Therefore,

$$c_1 \dot{x}_1 + c_2 \dot{x}_2 + \dots + c_{n-1} \dot{x}_{n-1} + c_n \dot{x}_n - C \dot{x}_d = -k \text{sat}(s)$$

$$\dot{s} = -k \text{sat}(s)$$

when $s > \Phi$

$$\dot{s} = -k$$

when $|s| < \Phi$

$$\dot{s} = -k s$$

Which means that the s value converge like a first order filter when the trajectory goes into the boundary layer.

The continuous sliding mode control was fully developed by many researchers and has been used in different ways in the industry field. We are going to discuss the properties of the sliding mode control in discrete time domain.

Discrete Time Controller Design

We consider a n -th order continuous nonlinear system in a canonical form and use the finite difference approximation to derive a discrete time system which contains modeling error on each approximation. The system dynamics equation could be in the form of

$$\mathbf{x}_1(k+1) = \mathbf{x}_1(k) + \Delta t \mathbf{x}_2(k) + \Delta t \mathbf{h}_1(k)$$

$$x_2(k+1) = x_2(k) + \Delta t x_3(k) + \Delta t h_2(k)$$

$$\vdots$$

$$x_n(k+1) = x_n(k) + \Delta t f(x_1, x_2, \dots, x_n) + \Delta t g(x_1, x_2, \dots, x_n) u(k) + \Delta t h_n(k)$$

where

$$\mathbf{H}(k) = [h_1(k), h_2(k), \dots, h_n(k)]^T$$

$\mathbf{H}(k)$ is the k-th modeling error vector

Define the sliding plane in the time k

$$s(k) = \mathbf{C} \tilde{\mathbf{x}}(k)$$

where

$$\mathbf{C} = [c_1, c_2, \dots, c_n] \quad c_i \neq 0, \quad i = 1, 2, \dots, n$$

$$\tilde{\mathbf{x}}(k) = \mathbf{x}(k) - \mathbf{x}_d(k)$$

(a) $\mathbf{x}(k)$ is the k-th measured trajectory

(b) $\mathbf{x}_d(k)$ is the k-th desired trajectory

Define

$$\begin{aligned} \Delta s(k) &= s(k+1) - s(k) \\ &= \mathbf{C} \tilde{\mathbf{x}}(k+1) - \mathbf{C} \tilde{\mathbf{x}}(k) \end{aligned}$$

Square method [24]

Since our intention here is to get $\mathbf{x}(k) = \mathbf{x}_d(k)$, we try to reduce the value of $s(k)$ in order to let the system reach the sliding surface and then slide down to the desired point.

That is,

$$s^2(k+1) < s^2(k)$$

We already know that

$$\Delta s(k) = s(k+1) - s(k)$$

Rearrange and square both sides

$$s^2(k+1) = s^2(k) + 2s(k)\Delta s(k) + \Delta s^2(k)$$

We want $s^2(k+1) < s^2(k)$ outside the sliding surface, and therefore the two terms of the right hand side should be negative

$$2s(k)\Delta s(k) + \Delta s^2(k) < 0$$

Since $s(k)$ is outside the sliding surface then $s(k) \neq 0$.

$$2 \frac{s(k)}{\Delta s(k)} + 1 < 0$$

$$\frac{s(k)}{\Delta s(k)} < -\frac{1}{2}$$

$$\frac{\Delta s(k)}{s(k)} > -2$$

If

$$s(k) > 0, \text{ then } 0 > \Delta s(k) > -2s(k) \quad (3)$$

$$s(k) < 0, \text{ then } 0 < \Delta s(k) < -2s(k) \quad (4)$$

Discrete time sliding mode control law

We know that

$$\Delta s(k) = C x(k+1) - C x(k) - C (x_d(k+1) - x_d(k)) =$$

$$c_1 x_1(k) + c_1 \Delta t x_2(k) + c_1 \Delta t h_1(k) + \dots + c_{n-1} x_{n-1}(k) + c_{n-1} \Delta t x_n(k) + c_{n-1} \Delta t h_{n-1}(k)$$

$$\begin{aligned}
& + c_n x_n(k) + c_n \Delta t f(x_1, x_2, \dots, x_n) + c_n \Delta t g(x_1, x_2, \dots, x_n) u(k) + c_n \Delta t h_n(k) \\
& - (c_1 x_1(k) + \dots + c_n x_n(k)) - C (x_d(k+1) - x_d(k))
\end{aligned}$$

If $s(k) > 0$

$0 >$

$$\begin{aligned}
& c_1 x_1(k) + c_1 \Delta t x_2(k) + c_1 \Delta t h_1(k) + \dots + c_{n-1} x_{n-1}(k) + c_{n-1} \Delta t x_n(k) + c_{n-1} \Delta t h_{n-1}(k) \\
& + c_n x_n(k) + c_n \Delta t f(x_1, x_2, \dots, x_n) + c_n \Delta t g(x_1, x_2, \dots, x_n) u(k) + c_n \Delta t h_n(k) \\
& - (c_1 x_1(k) + \dots + c_n x_n(k)) - C (x_d(k+1) - x_d(k)) > -2 s(k)
\end{aligned}$$

which is

$$\begin{aligned}
0 > \Delta t (c_1 x_2(k) + \dots + c_{n-1} x_n(k)) + \Delta t C H(k) + c_n \Delta t f(x_1, x_2, \dots, x_n) \\
& + c_n \Delta t g(x_1, x_2, \dots, x_n) u(k) - C (x_d(k+1) - x_d(k)) > -2 s(k)
\end{aligned}$$

$$p - \frac{1}{c_n g} C H(k) > u(k) > p - \frac{2}{\Delta t c_n g} s(k) - \frac{1}{c_n g} C H(k)$$

Let

$$u = p - q \operatorname{sat} \left(\frac{s(k)}{\Phi} \right)$$

where

$$\begin{aligned}
p & = -\frac{1}{c_n g} (c_1 x_2(k) + \dots + c_{n-1} x_n(k)) - \frac{1}{g} f(x_1, x_2, \dots, x_n) \\
& + \frac{1}{\Delta t c_n g} C (x_d(k+1) - x_d(k))
\end{aligned}$$

$$\frac{1}{c_n g} C H(k) < q < \frac{2}{\Delta t c_n g} s(k) + \frac{1}{c_n g} C H(k)$$

$$\text{sat}(s(k)) = \left\{ \begin{array}{l} \frac{s(k)}{|s(k)|} = \text{sgn}(s(k)) \text{ for } |s(k)| \geq \Phi \\ \frac{s(k)}{\Phi} \text{ for } |s(k)| < \Phi \end{array} \right\}$$

$$\Phi > \gamma$$

Assume that the modeling error is bounded in some certain value. we get

$$\frac{1}{c_n g} C H(k) \in [-\gamma, \gamma]$$

let

$$q = \left\{ \begin{array}{l} \alpha \frac{1}{\Delta t c_n g} |s(k)| + \gamma \text{ when } |s(k)| > \Phi \\ \alpha \frac{1}{\Delta t c_n g} \Phi + \gamma \text{ when } |s(k)| < \Phi \end{array} \right\} \quad 0 < \alpha < 2$$

The $u(k)$ is the discrete time sliding mode control law.

Stability analysis

Plugging in the control law to the dynamics equation, we get

$$x_n(k+1) = x_n(k) + \Delta t f(x_1, \dots, x_n) + \Delta t h_n(k)$$

$$+ \Delta t g \left(-\frac{1}{c_n g} (c_1 x_2(k) + \dots + c_{n-1} x_n(k)) - \frac{1}{g} f(x_1, \dots, x_n) + \frac{1}{\Delta t c_n g} C (x_d(k+1) - x_d(k)) \right)$$

$$- \left(\frac{\alpha}{\Delta t c_n g} s(k) + \gamma \right) \text{sat} (s(k))$$

Reaching phase

When the trajectory is outside the boundary, $s(k) > \Phi$, we call it reaching phase. The Square Method can guarantee the sliding surface is attractive because of the Lyapunov equation. The distance between the trajectory and sliding surface is decayed with respect to time outside the boundary layer.

Inside the boundary layer

$$x_n(k+1) = x_n(k) - \frac{\Delta t}{c_n} (c_1 x_2(k) + \dots + c_{n-1} x_n(k)) - \frac{\alpha}{c_n} (c_1 x_1(k) + \dots + c_n x_n(k))$$

$$- \frac{g \Delta t \gamma}{\Phi} s(k) + \Delta t h_n(k) + \frac{1}{c_n} C (x_d(k+1) - x_d(k))$$

$$x_n(k+1) = - \frac{1}{c_n} (C x(k+1) - C x(k) - \Delta t C H(k)) + x_n(k+1) - \frac{\alpha}{c_n} C x(k)$$

$$- \frac{g \Delta t \gamma}{\Phi} C x(k) + \frac{g \Delta t \gamma}{\Phi} C x_d(k) + \frac{1}{c_n} C (x_d(k+1) - x_d(k))$$

Therefore

$$\begin{aligned}
& -\frac{1}{c_n} C x(k+1) + \frac{(1 - \alpha - \frac{g \Delta t \gamma}{\Phi})}{c_n} C x(k) \\
& + \frac{1}{c_n} \Delta t C H(k) + \frac{g \Delta t \gamma}{\Phi} C x_d(k) + \frac{1}{c_n} C (x_d(k+1) - x_d(k)) = 0 \\
\frac{1}{c_n} s(k+1) - \frac{(1 - \alpha - \frac{g \Delta t \gamma}{\Phi})}{c_n} s(k) & = F_1(k)
\end{aligned}$$

where

$$F_1(k) = -\frac{1}{c_n} \Delta t C H(k) + \frac{(\alpha + \frac{g \Delta t \gamma}{\Phi})}{c_n} C x_d(k)$$

Using Z-transform we get

$$\frac{1}{c_n} (z - (1 - \alpha - \frac{g \Delta t \gamma}{\Phi})) s(z) = F_1(z)$$

The limitation of stability is

$$0 < \alpha < 2 - \frac{g \Delta t \gamma}{\Phi}$$

Similarly, when the $s(k) < -\Phi$ we get the same result.

With all the derivations presented above in a canonical form, This study will examine the effects of those theorem to a **SCARA** robot model.

Model Description

Introduction

We are analyzing the relationship between the actuator torque and joint angular acceleration for a device with two degrees of freedom, such as arm on a lathe machine. The method presents here utilizes the Euler-Lagrange equation. We use this method to provide a clear understanding of the effect of varying inertia, joint interaction, and coriolis force. It also forms the basis of simulation of such a system and, most importantly, design of control system.

Two-link Robot Model

A two-degree-of-freedom robot arm manipulator is equipped at each joint with an actuator DC motor to provide input torque, an encoder for measuring joint position, and a tachometer for measuring joint velocity. Fig 10 shows the outlook of the system.

The dynamic equation of the SCARA robot, derived in Appendix A, is a second nonlinear differential equation in the form of

$$\mathbf{J} \ddot{\mathbf{q}} + \mathbf{C} \dot{\mathbf{q}} + \mathbf{g} = \mathbf{\Gamma}$$

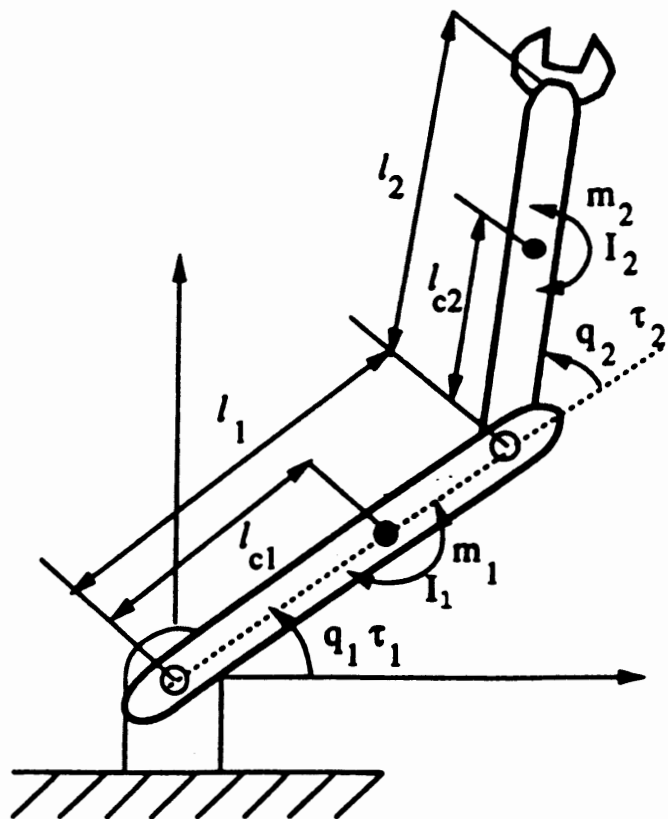


Figure 10. The Model of SCARA Robot

where

$$\mathbf{J} = \begin{bmatrix} J_{11} & J_{12} \\ J_{21} & J_{22} \end{bmatrix}$$

$$J_{11} = J_1 + J_2 + M_1 l_1^2 + M_2 (L_1^2 + l_2^2 + 2L_1 l_2 \cos q_2)$$

$$J_{12} = M_2 (l_2^2 + L_1 l_2 \cos q_2) + J_2$$

$$J_{21} = M_2 (l_2^2 + L_1 l_2 \cos q_2) + J_2$$

$$J_{22} = M_2 l_2^2 + J_2$$

$$\mathbf{C} = \begin{bmatrix} -2M_2 L_1 l_2 \sin q_2 \dot{q}_2 & -2M_2 L_1 l_2 \sin q_2 \dot{q}_2 \\ M_2 L_1 l_2 \sin q_2 \dot{q}_1 & 0 \end{bmatrix}$$

$$\mathbf{g} = \begin{bmatrix} g(M_1 l_1 + M_2 l_1) \sin q_1 + g(M_2 l_2 \sin (q_1 + q_2)) \\ gM_2 l_2 \sin (q_1 + q_2) \end{bmatrix}$$

$$\mathbf{\Gamma} = \begin{bmatrix} \Gamma_{1 \text{ actuator}} - \Gamma_{1 \text{ friction}} \\ \Gamma_{2 \text{ actuator}} - \Gamma_{2 \text{ friction}} \end{bmatrix}$$

To check the equation derived above, we simply give the robot arm some initial conditions and add a constant friction in both joints to check whether the total energy decreases all the way down. The ideal friction force Γ_{friction} between each joint in matrix form is

$$\mathbf{\Gamma}_{\text{friction}} = \begin{bmatrix} a & b \\ -b & 0 \end{bmatrix} \begin{bmatrix} \dot{\theta}_1 \\ \dot{\theta}_2 \end{bmatrix}$$

The results are shown in figure 11 . The total energy goes down all the way to the equilibrium point. The 1st and 2nd link go to the zero point after a period of time.

The implementation of discrete time sliding mode control to SCARA robot will be discussed in the next chapter.

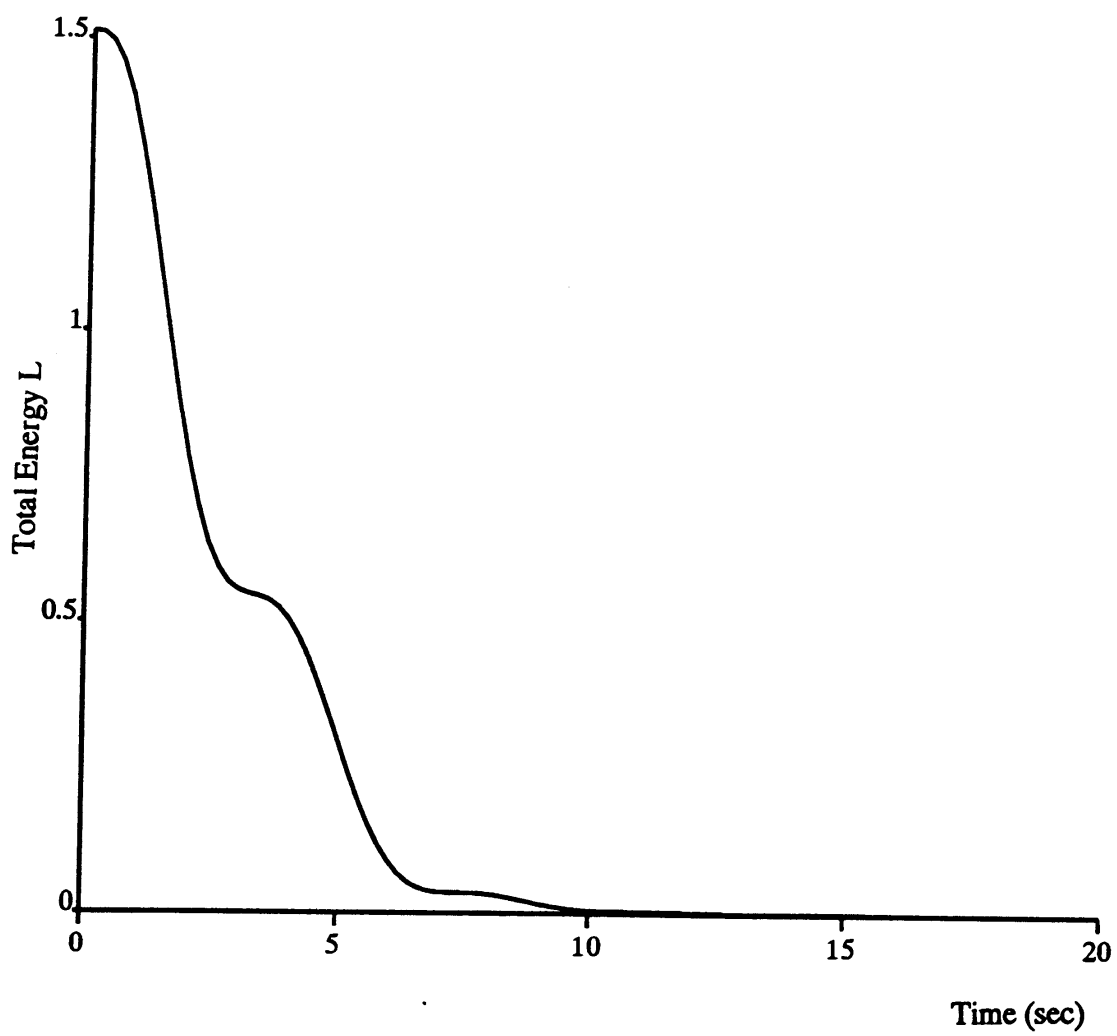


Figure 11. Model Checking Simulation

CHAPTER IV

SIMULATIONS AND RESULTS

Application to a SCARA Robot

From the appendix A, the SCARA robot dynamics could be in the form of

$$\mathbf{J} \ddot{\mathbf{x}} + \mathbf{C} \dot{\mathbf{x}} = \mathbf{f}$$

where

$$\mathbf{J} = \begin{bmatrix} J_{11} & J_{12} \\ J_{21} & J_{22} \end{bmatrix}$$

$$J_{11} = J_1 + J_2 + M_1 l_1^2 + M_2 (L_1^2 + l_2^2 + 2L_1 l_2 \cos x_2)$$

$$J_{12} = M_2 (l_2^2 + L_1 l_2 \cos x_2) + J_2$$

$$J_{21} = M_2 (l_2^2 + L_1 l_2 \cos x_2) + J_2$$

$$J_{22} = M_2 l_2^2 + J_2$$

$$\mathbf{C} = \begin{bmatrix} -2M_2 L_1 l_2 \sin x_2 \dot{x}_2 & -2M_2 L_1 l_2 \sin x_2 \dot{x}_2 \\ M_2 L_1 l_2 \sin x_2 \dot{x}_1 & 0 \end{bmatrix}$$

$$\mathbf{f} = \begin{bmatrix} f_1 \\ f_2 \end{bmatrix}$$

The numerical value we give to the system are

$$J_1 = 10, J_2 = 5, M_1 = 1, M_2 = 0.5, L_1 = 1, l_1 = 0.5, l_2 = 0.3$$

Implementation of Discrete Sliding Mode Control

Let us define a sliding surface in discrete time domain as

$$s(k) = \tilde{\dot{x}}(k) + \lambda \tilde{x}(k)$$

The desired trajectories are

$$x_{1d}(k) = -\cos(kT) \quad k = 1, 2, 3, \dots$$

$$x_{2d}(k) = 2 - \cos(kT) \quad k = 1, 2, 3, \dots$$

Where T is the sampling period.

Uncertain System

During the modeling process there are approximations and uncertainties which could, in some cases, cause the system to be unstable. We will consider the perturbation of the control system in the modeling process.

We know that acceleration is the rate of velocity change, and that modeling compels errors. We could express as

$$\ddot{x}(k) = \frac{\dot{x}(k+1) - \dot{x}(k)}{\Delta t} + h_2(k)$$

We don't know what exactly $h_2(k)$ is but we know that it is bounded. Combining with system equation we have

$$\dot{\mathbf{x}}(k+1) - \dot{\mathbf{x}}(k) = \Delta t \mathbf{J}^{-1} (-\mathbf{C}\dot{\mathbf{x}} + \mathbf{f}) + \Delta \mathbf{f}$$

where $\Delta \mathbf{f} = \Delta t h_2(k) + \psi + \mathbf{d}$

ψ is parameters uncertainties

\mathbf{d} is disturbances

Assume we know the upper bound of $\Delta \mathbf{f}$, which means

$$\Delta \mathbf{f} \in [-\gamma, \gamma]$$

From the square method that we previously mentioned, the changing rate of $s(k)$ should be in the relationship like

If

$$s(k) > 0, \quad \text{then } 0 > \Delta s(k) > -2s(k)$$

$$s(k) < 0, \quad \text{then } 0 < \Delta s(k) < -2s(k)$$

In another word, when $s(k) > 0$

$$\Delta s(k) = -\Delta t \mathbf{J}^{-1} \mathbf{C} \dot{\mathbf{x}} + \Delta t \mathbf{J}^{-1} \mathbf{f} - \Delta t \mathbf{J}^{-1} \Delta v_d(k) + \lambda \Delta t \mathbf{J}^{-1} \Delta \tilde{\mathbf{x}}(k) - \Delta t h_2(k)$$

$$0 > -\Delta t \mathbf{J}^{-1} \mathbf{C} \dot{\mathbf{x}} + \Delta t \mathbf{J}^{-1} \mathbf{f} - \Delta t \mathbf{J}^{-1} \Delta v_d(k) + \lambda \Delta t \mathbf{J}^{-1} \Delta \tilde{\mathbf{x}}(k) - \Delta t h_2(k) > -2s(k)$$

Which means

$$\mathbf{f} < \mathbf{C}\dot{\mathbf{x}} + \frac{1}{\Delta t} \mathbf{J} \Delta v_d(k) - \frac{1}{\Delta t} \lambda \mathbf{J} \Delta \tilde{\mathbf{x}}(k)$$

$$\mathbf{f} > \mathbf{C}\dot{\mathbf{x}} + \frac{1}{\Delta t} \mathbf{J} \Delta v_d(k) - \frac{1}{\Delta t} \lambda \mathbf{J} \Delta \tilde{\mathbf{x}}(k) - \frac{2}{\Delta t} \mathbf{J} s(k) - \frac{1}{\Delta t} \mathbf{J} \Delta \mathbf{f}$$

When $S(k) < 0$

$$0 < -\Delta t \mathbf{J}^{-1} \mathbf{C} \dot{\mathbf{x}} + \Delta t \mathbf{J}^{-1} \mathbf{f} - \Delta t \mathbf{J}^{-1} \Delta \mathbf{v}_d(\mathbf{k}) + \lambda \Delta t \mathbf{J}^{-1} \Delta \tilde{\mathbf{x}}(\mathbf{k}) - \Delta t \mathbf{h}_2(\mathbf{k}) < -2 \mathbf{s}(\mathbf{k})$$

Which means

$$\mathbf{f} > \mathbf{C} \dot{\mathbf{x}} + \frac{1}{\Delta t} \mathbf{J} \Delta \mathbf{v}_d(\mathbf{k}) - \frac{1}{\Delta t} \lambda \mathbf{J} \Delta \tilde{\mathbf{x}}(\mathbf{k})$$

$$\mathbf{f} < \mathbf{C} \dot{\mathbf{x}} + \frac{1}{\Delta t} \mathbf{J} \Delta \mathbf{v}_d(\mathbf{k}) - \frac{1}{\Delta t} \lambda \mathbf{J} \Delta \tilde{\mathbf{x}}(\mathbf{k}) - \frac{2}{\Delta t} \mathbf{J} \mathbf{s}(\mathbf{k}) - \frac{1}{\Delta t} \mathbf{J} \Delta \mathbf{f}$$

Let

$$\mathbf{f} = \mathbf{P} - \mathbf{Q} \text{sat}(\mathbf{s}(\mathbf{k}))$$

where

$$\mathbf{P} = \mathbf{C} \dot{\mathbf{x}} + \frac{1}{\Delta t} \mathbf{J} \Delta \mathbf{v}_d(\mathbf{k}) - \frac{1}{\Delta t} \lambda \mathbf{J} \Delta \tilde{\mathbf{x}}(\mathbf{k})$$

$$\frac{\mathbf{J}}{\Delta t} \gamma < \mathbf{Q} < \left(\frac{\mathbf{J}}{\Delta t} \gamma + \frac{2\mathbf{J}}{\Delta t} \mathbf{s}(\mathbf{k}) \right) \quad (5)$$

let

$$\mathbf{Q} = \begin{cases} \alpha \frac{\mathbf{J}}{\Delta t} |\mathbf{s}(\mathbf{k})| + \frac{\mathbf{J}}{\Delta t} \gamma & \text{when } |\mathbf{s}(\mathbf{k})| > \Phi \\ \alpha \frac{\mathbf{J}}{\Delta t} \Phi + \frac{\mathbf{J}}{\Delta t} \gamma & \text{when } |\mathbf{s}(\mathbf{k})| < \Phi \end{cases} \quad 0 < \alpha < 2$$

From (5) we know that the $\mathbf{s}(\mathbf{k})$ should have limitations as

$$\left(\frac{\mathbf{J}}{\Delta t} \gamma + \frac{2\mathbf{J}}{\Delta t} \mathbf{s}(\mathbf{k}) \right) > \mathbf{Q}$$

$$\left(-\frac{\mathbf{J}}{\Delta t} \gamma + \frac{2\mathbf{J}}{\Delta t} \mathbf{s}(\mathbf{k}) \right) > \mathbf{Q}$$

Therefore, the worst case to guarantee $\mathbf{s}(\mathbf{k}) > 0$ is

$$s(k) > \frac{\Delta t \mathbf{J}^{-1}}{2} \left(\frac{-\mathbf{J}}{\Delta t} \gamma + \mathbf{Q} \right)$$

We can define the boundary layer Φ :

$$\Phi > \frac{\Delta t}{2} \mathbf{J}^{-1} \left(\frac{-\mathbf{J}}{\Delta t} \gamma + \mathbf{Q} \right)$$

Plugging in \mathbf{Q} we know that

$$\Phi > \frac{\Delta t}{2} \mathbf{J}^{-1} \left(\frac{-\mathbf{J}}{\Delta t} \gamma + \alpha \frac{-\mathbf{J}}{\Delta t} |s(k)| + \frac{-\mathbf{J}}{\Delta t} \gamma \right)$$

$$\Phi > \gamma + \frac{\alpha}{2} s(k), \quad \text{for } s(k) > 0$$

The constraint of the boundary layer is $\Phi > \gamma$ which results in the same conclusion as Pieper and Surgenor [23] 1992.

Stability Analysis

Reaching Phase

Substituting the control input into the system dynamics when outside the boundary layer, we call a reaching phase. The square Method can guarantee the attractiveness of the trajectory to the sliding surface.

Inside the boundary layer

Substituting the control input into the system dynamics when inside the boundary layer,

$$v(k+1) - v(k) = \Delta \dot{x}_d(k) - \lambda \Delta \tilde{x}(k) - \alpha s(k) - \frac{\gamma}{\Phi} s(k) + \Delta t h_2(k)$$

$$s(k+1) - s(k) = - \left(\alpha + \frac{\gamma}{\Phi} \right) s(k) + \Delta t h_2(k)$$

$$s(z) = \frac{- \Delta t h_2(z)}{\left(z - \left(1 - \alpha - \frac{\gamma}{\Phi} \right) \right)}$$

The stability condition should be

$$0 < \alpha + \frac{\gamma}{\Phi} < 2$$

From the state space point of view to consider the system stability

$$v(k+1) - v(k) = \Delta \dot{x}_d(k) - \lambda \Delta \tilde{x}(k) - \left(\alpha + \frac{\gamma}{\Phi} \right) s(k) + \Delta t h_2(k)$$

$$v(k+1) = (1 - \beta) v(k) - (1 + \beta) \lambda x(k) + \lambda x(k-1) + u(k)$$

where

$$\beta = \alpha + \frac{\gamma}{\Phi}$$

$$u(k) = \Delta v_d(k) + \beta v_d(k) + \beta \lambda x_d(k) + \Delta t h_2(k)$$

$$(z - (1 - \beta)) v(z) = \frac{-(1 + \beta) \lambda z + \lambda}{z} x(z) + u(z)$$

$$(z - 1) x(z) = \Delta t v(z) + \Delta t h_1(k)$$

$$(z - 1) x(z) = \frac{\Delta t (-(1 + \beta) \lambda z + \lambda)}{z (z - (1 - \beta))} x(z) + \frac{\Delta t}{(z - (1 - \beta))} u(z) + \Delta t h_1(z)$$

$$x(z) = \frac{z (z - (1 - \beta))}{z^3 - (2 - \beta) z^2 + (1 - \beta + \lambda \Delta t + \lambda \Delta t \beta) z - \lambda \Delta t} u_1(z)$$

where

$$u_1(z) = \frac{\Delta t}{(z - (1 - \beta))} u(z) + \Delta t h_1(z)$$

The stability ability is related with the choice of β and $\lambda \Delta t$. The β dominates the precision of the steady state error. Significantly the $\lambda \Delta t$ will effect the system's stability because of the location of poles. It is interesting that we need some trade off between λ and Δt . However, if we want a larger λ , we have to choose a smaller sampling time or vice versa.

We pick $\beta = 1$ and plot the root locus of the system under the change of $\lambda \Delta t$ as shown in figure 12.

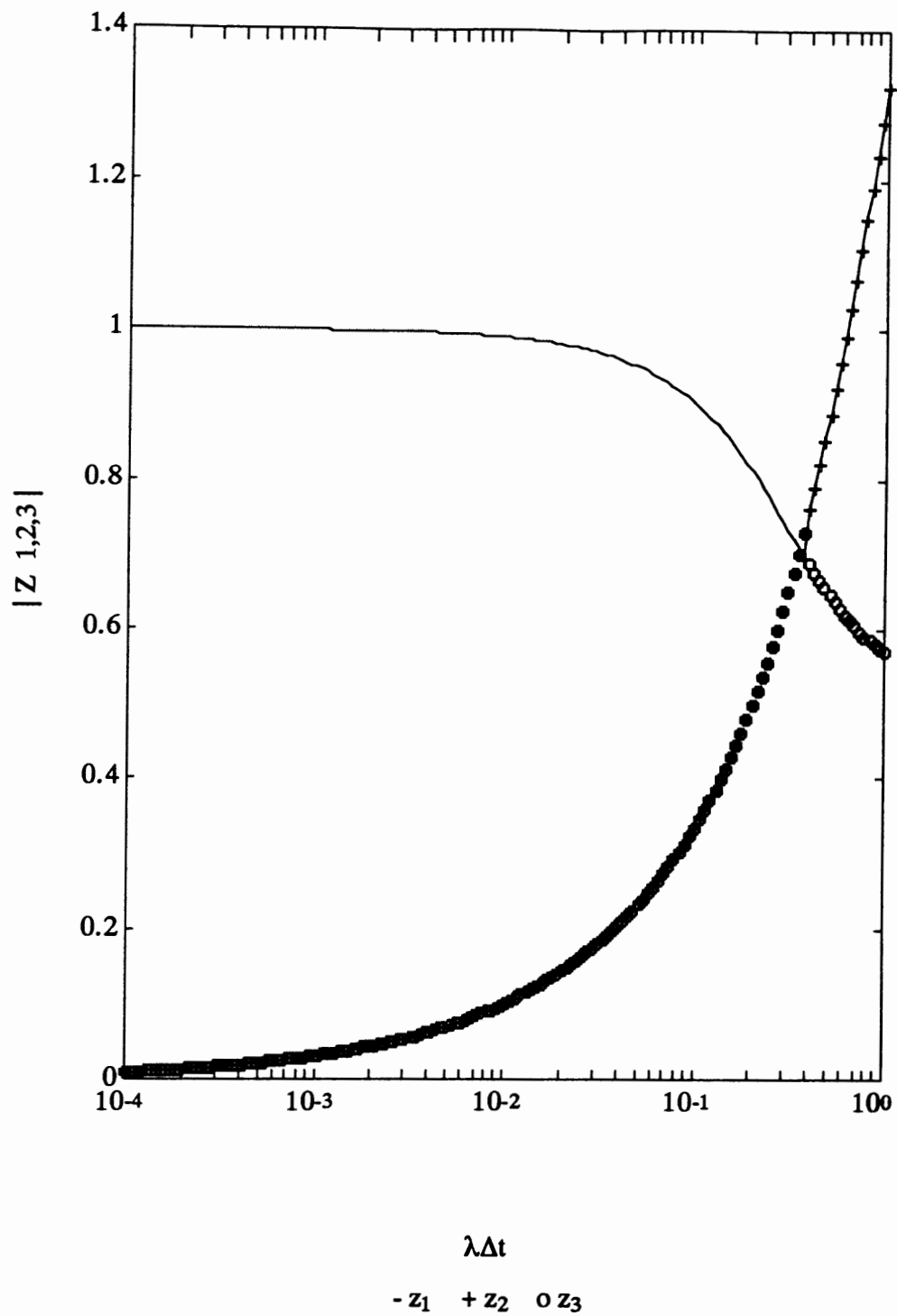


Figure 12: The root locus of discrete time sliding mode control for SCARA robot
with $\beta = 1$

Simulation Discussions

We use the numerical value of $\gamma = 0.01$ and choose the boundary layer thickness $\Phi = 0.02$. Therefore, α equals 0.5 which is satisfied by the stability restrictions of the reaching phase and inside the boundary layer.

Also, according to the pole's location in Figure [12], we use the reaching rate $\lambda = 5$ and use different sampling rates (0.01, 0.05 and 0.2) to simulate the system that gets the results shown in Figures [13]-[34]. Figures [13]-[18] show the simulations of the sampling time $\Delta t = 0.01$ where $\lambda\Delta t = 0.05$ locates the poles within the unit circle as shown in figure 12. The results in these figures show a stable system from the simulation.

Effect of Sampling Time

With the sampling time $\Delta t = 0.05$, the product of $\lambda\Delta t = 0.25$ locates the poles within unit circle too, but it goes with a slower convergent rate than $\Delta t = 0.01$ because of the roots' location as shown in Figures [19]-[24]. However, when the sampling time is larger than the boundary layer thickness, $s(k)$ will cause chattering in the neighborhood of the sliding surface.

When the sampling time $\Delta t = 0.2$, the product of $\lambda\Delta t = 1$ locates the system's poles outside the unit circle. Whatever the value of α be chosen, the system is still diverge as show in Figure [25]-[28].

The restrictions of choosing a sampling time to make a stable system in the discrete time sliding mode control are dependent on β , α , upper bound of disturbances and

modeling errors γ , boundary layer thickness Φ , and reaching rate λ . β and α are the stability factors of the $s(k)$. They will control the convergent rate of $s(k)$ and should be in their own specific range such that they could achieve a stable system.

Effect of Boundary Layer Thickness

The definition of boundary layer thickness Φ is important in the discrete time sliding mode control. Because the sliding mode control has the ability of robustness it can tolerate the modeling errors and disturbances. As long as we know the upper bound of the modeling errors and disturbances γ , the boundary layer thickness Φ should be chosen greater than γ in order to achieve the robust systems.

However, the choice of the sampling time Δt cannot be greater than the boundary layer thickness even if it is satisfied by the location of poles. When the sampling time is larger than the boundary layer thickness, the trajectory of s will never come into the boundary layer and will not converge to one specific small value. The behavior of trajectory across the sliding surface will be like a chattering of teeth and will never go to the desired point as shown in Figures [19]-[24].

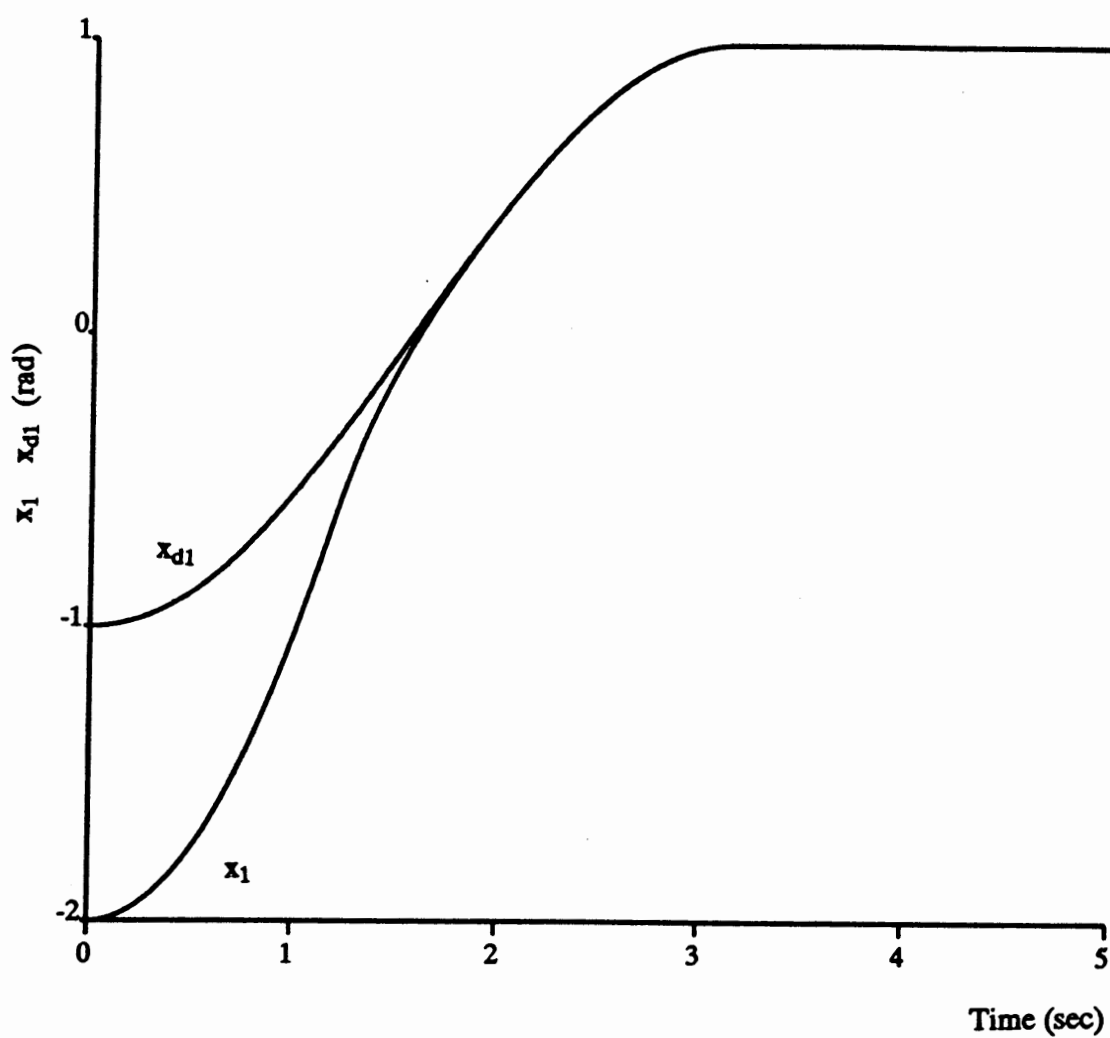
On the other hand if the boundary layer thickness is not smaller than the sampling time, there still will be a chance to eliminate the chattering effect and reach the desired point. As shown in Figure [29]-[34], using $\lambda = 10$, $\Delta t = 0.05$ and $\Phi = 0.05$ will eliminate the chattering and achieve the tracking error $s(k)$ asymptotically convergent to zero. This research basically recommends that the sampling time should be better if it is smaller than one half of the boundary layer thickness to get a better steady state error convergence.

Trade off Between Reaching Rate and Sampling Time

Another factor of stability is the trade off between λ and Δt . Sometimes, we only concentrate on using a sampling time as small as possible. However, sampling time is not a sufficient condition for the system's stability. From the poles' equation and the roots location figure, one could know the relationship between λ and Δt .

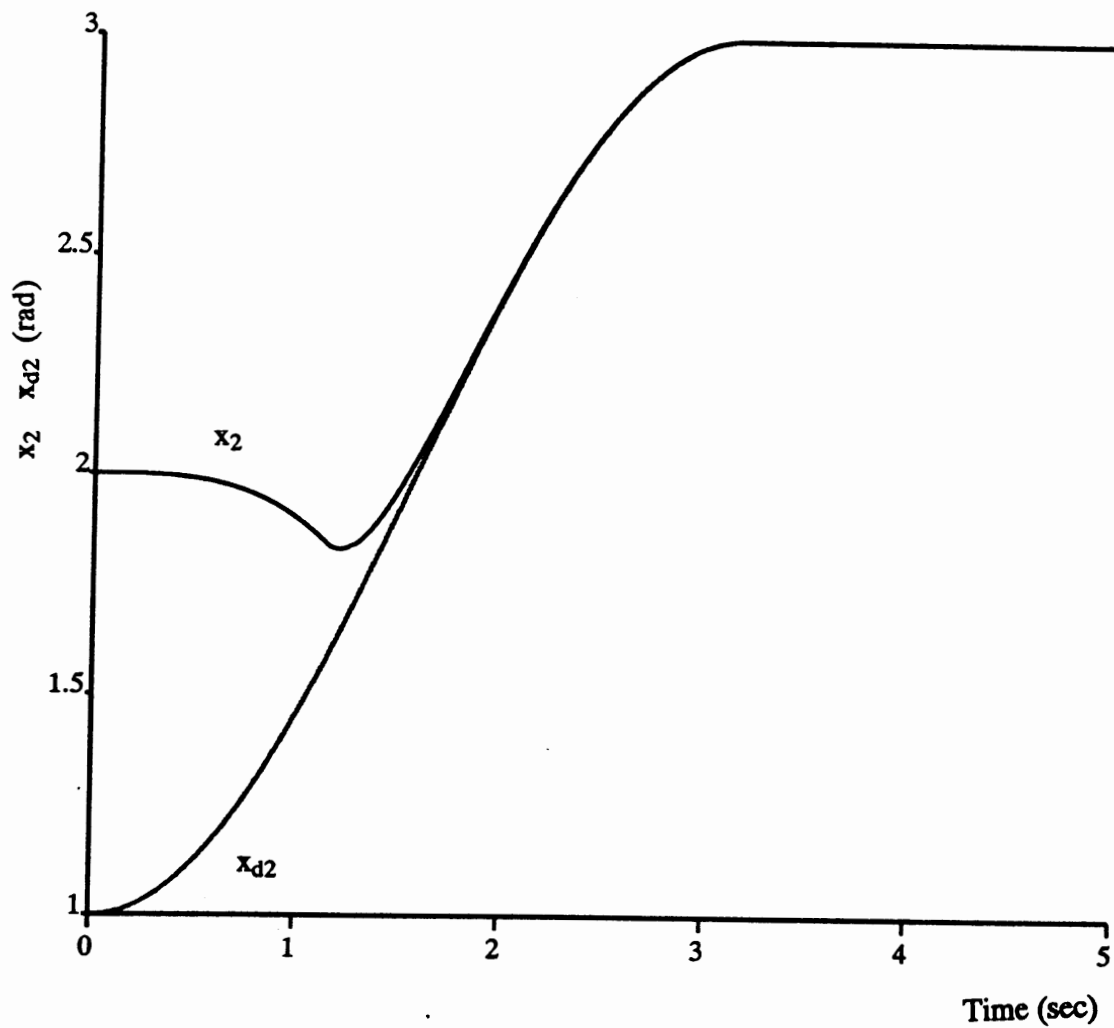
From the simulation results in Figure [35]-[40], using $\lambda = 50$, $\Delta t = 0.02$ and $\Phi = 0.05$, we obtain an unstable system even if we already use a small sampling time. Therefore, a small sampling time can not guarantee the system's stability, especially inside the boundary layer, when people use sliding mode control in a digital computer.

This research is dedicated to the design of the discrete time sliding mode control with control law derivation and stability analysis. In this paper, the author implements discrete time sliding mode control to a SCARA robot and discusses the stability that is affected by different parameters. People usually know that the sampling time should be as small as possible in order to behave as a continuous controller. Correspondingly, the cost of the product will be higher and money may be wasted to build up a controller with a quick sampling rate. An additional problem, during the sampling period, is that the behavior of the system is not known. Therefore, I address this problem and provide a cost efficient and user friendly way to construct a discrete time sliding mode control in the use of the digital computer.



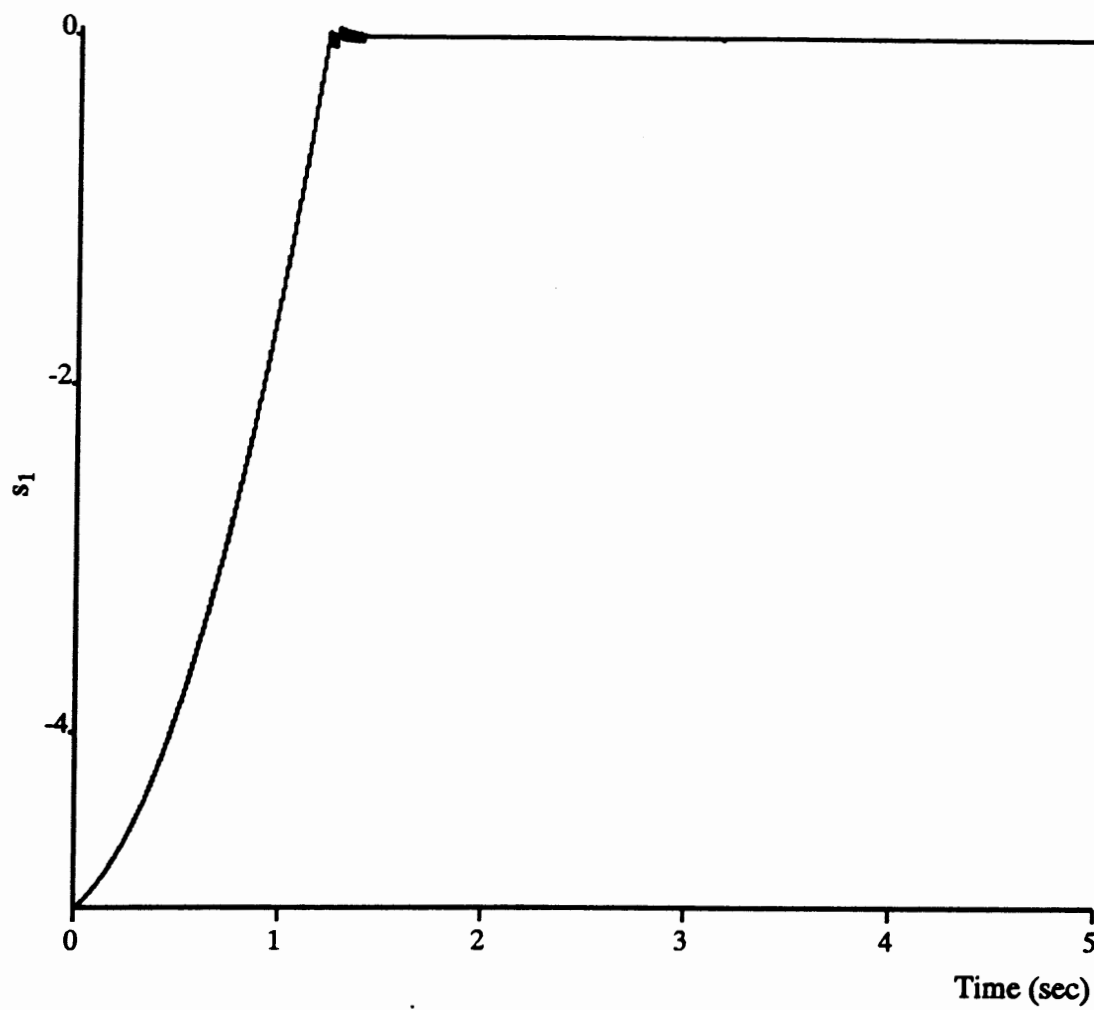
$$\lambda = 5 \quad \Delta t = 0.01 \quad \Phi = 0.02 \quad \gamma = 0.01 \quad \alpha = 0.5 \quad \beta = 1$$

Figure 13. 1-st Link Trajectory and Desired Trajectory



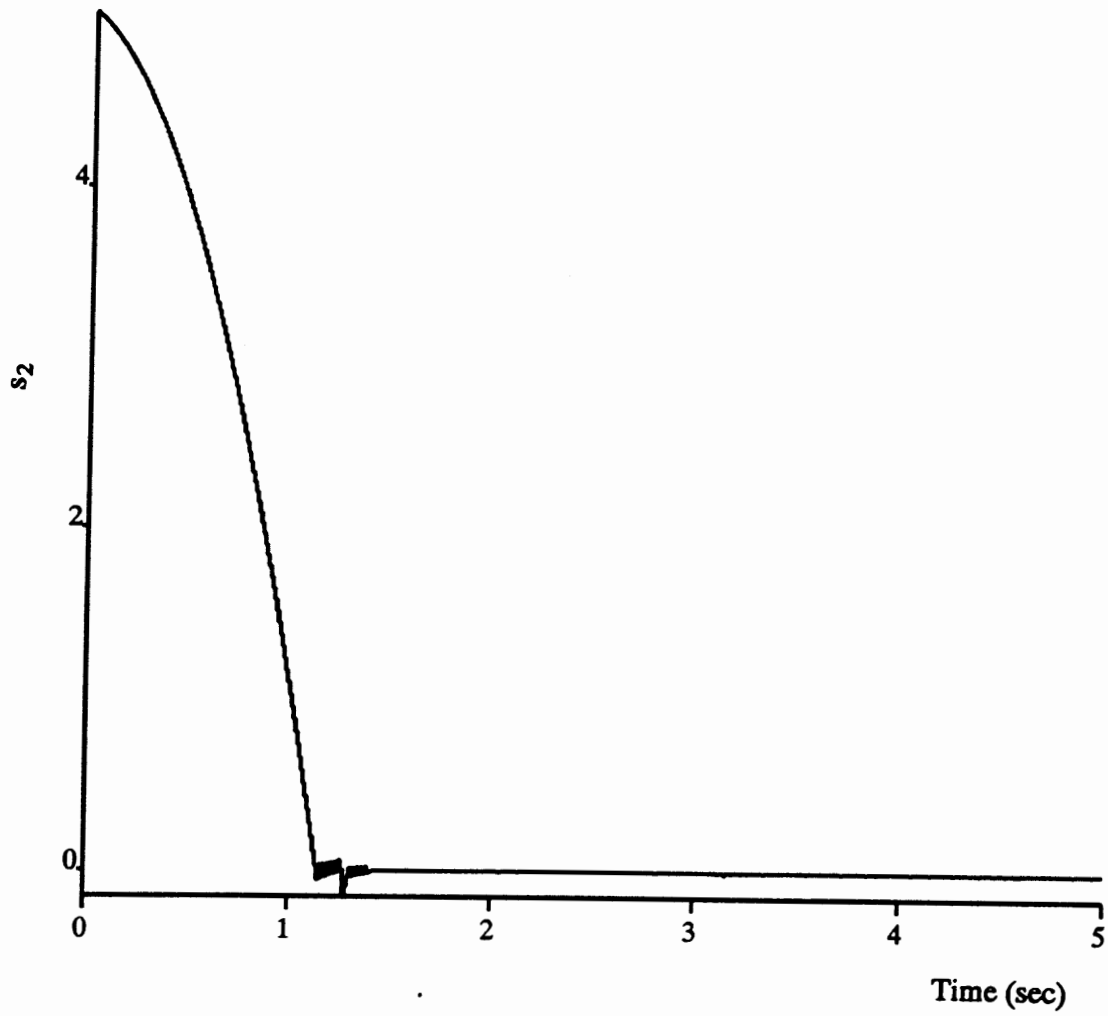
$$\lambda = 5 \quad \Delta t = 0.01 \quad \Phi = 0.02 \quad \gamma = 0.01 \quad \alpha = 0.5 \quad \beta = 1$$

Figure 14. 2-nd Link Trajectory and Desired Trajectory



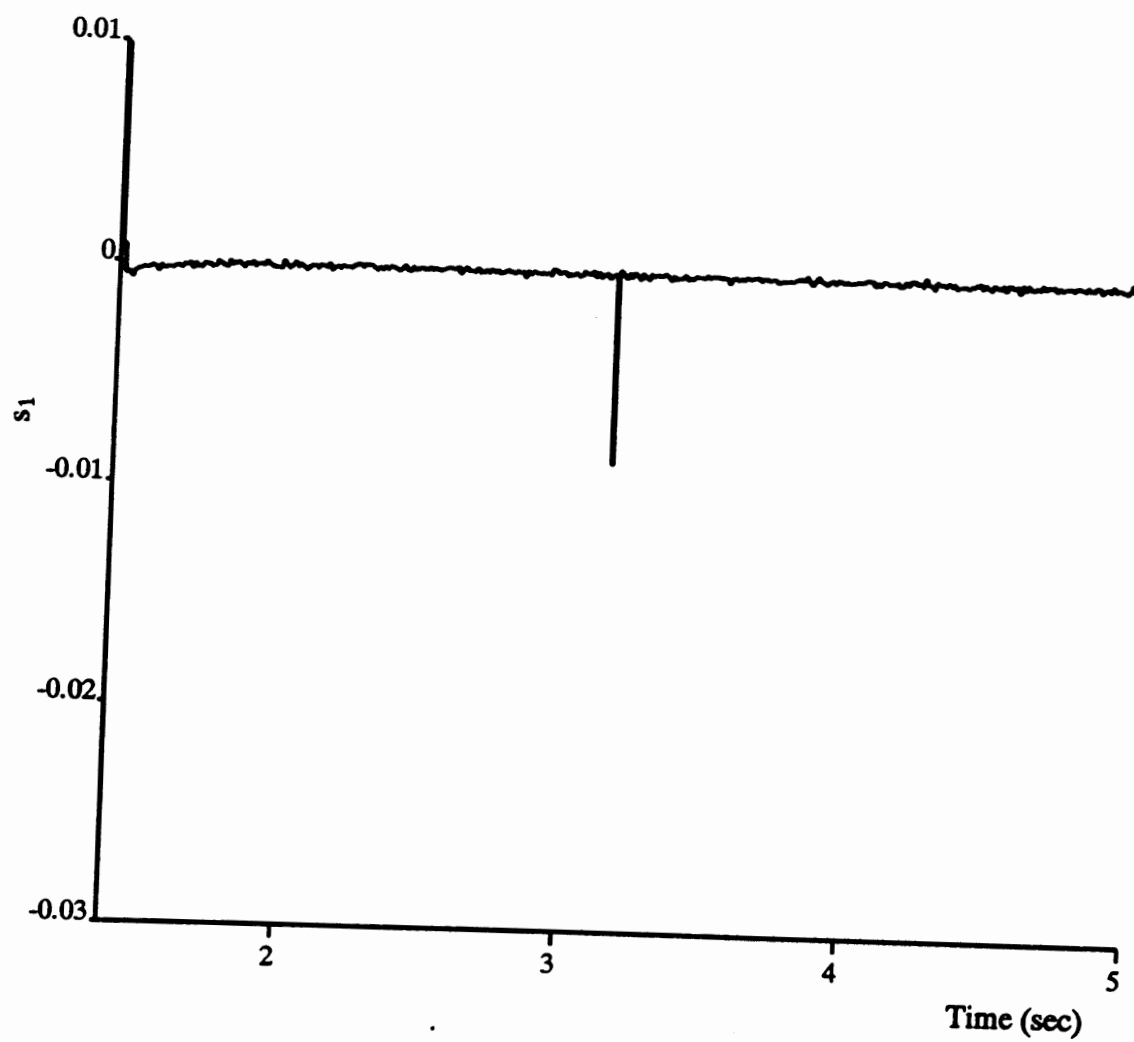
$$\lambda = 5 \quad \Delta t = 0.01 \quad \Phi = 0.02 \quad \gamma = 0.01 \quad \alpha = 0.5 \quad \beta = 1$$

Figure 15. $s_1(k)$



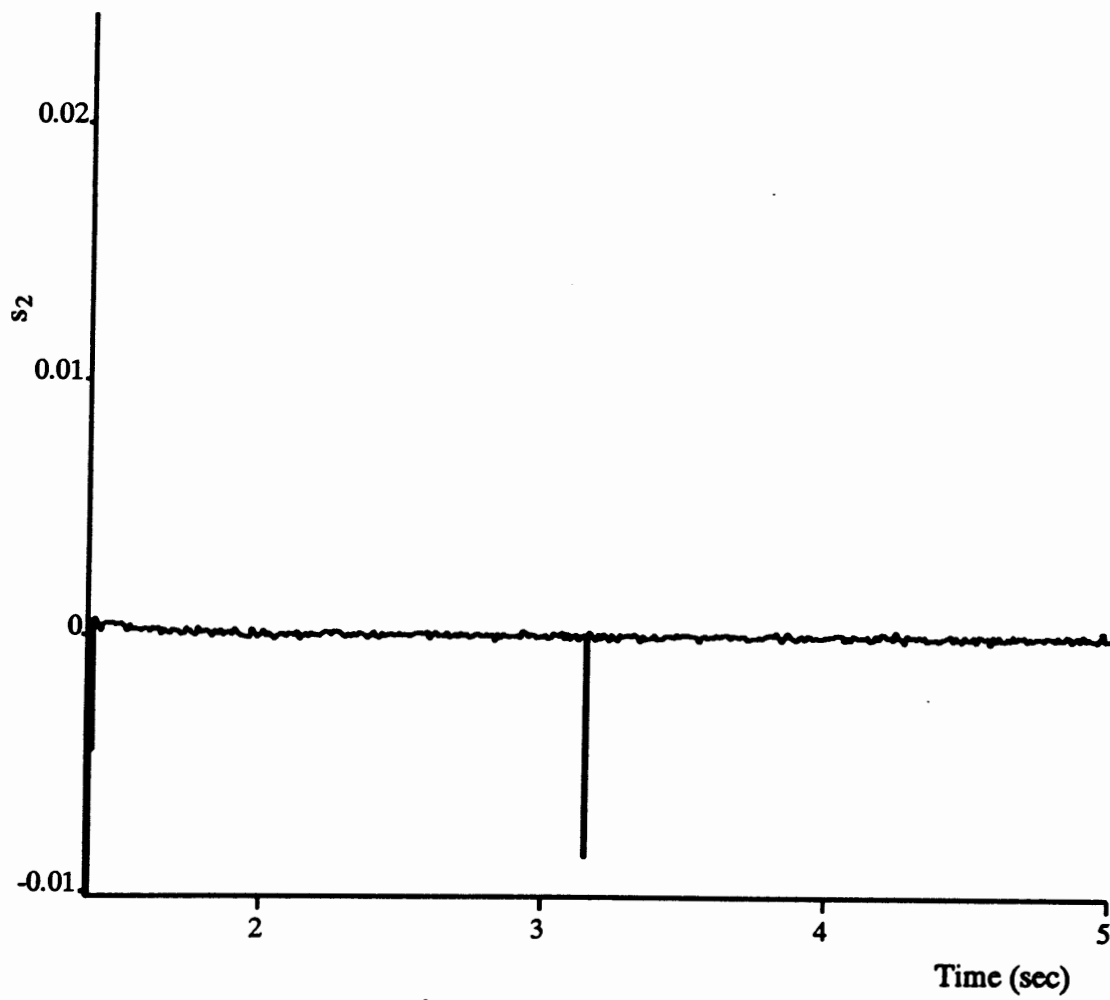
$$\lambda = 5 \quad \Delta t = 0.01 \quad \Phi = 0.02 \quad \gamma = 0.01 \quad \alpha = 0.5 \quad \beta = 1$$

Figure 16. $s_2(k)$



$$\lambda = 5 \quad \Delta t = 0.01 \quad \Phi = 0.02 \quad \gamma = 0.01 \quad \alpha = 0.5 \quad \beta = 1$$

Figure 17. Zooming of $s_1(k)$



$$\lambda = 5 \quad \Delta t = 0.01 \quad \Phi = 0.02 \quad \gamma = 0.01 \quad \alpha = 0.5 \quad \beta = 1$$

Figure 18. Zooming of $s_2(k)$

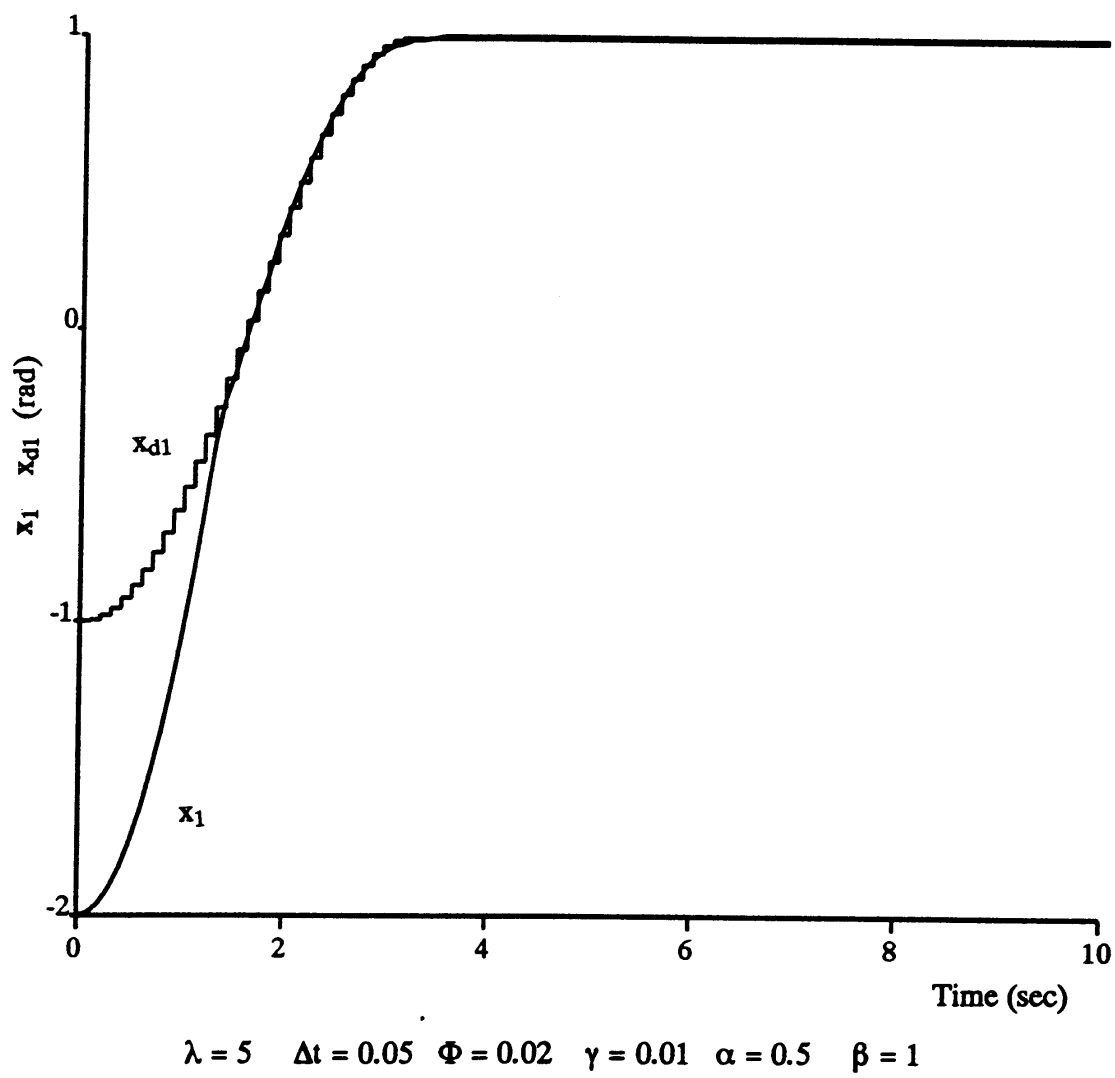


Figure 19. 1-st Link Trajectory and Desired Trajectory

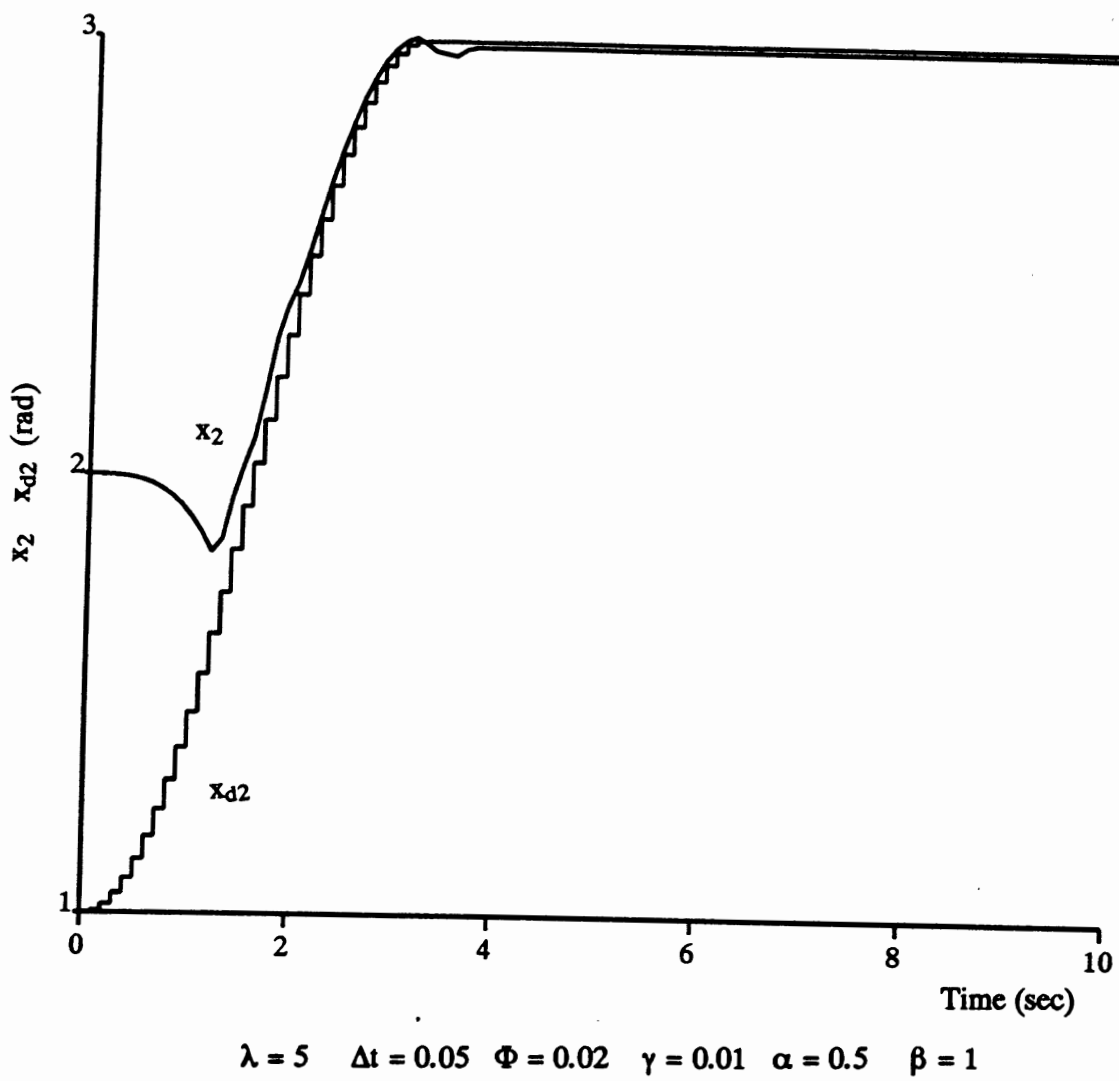
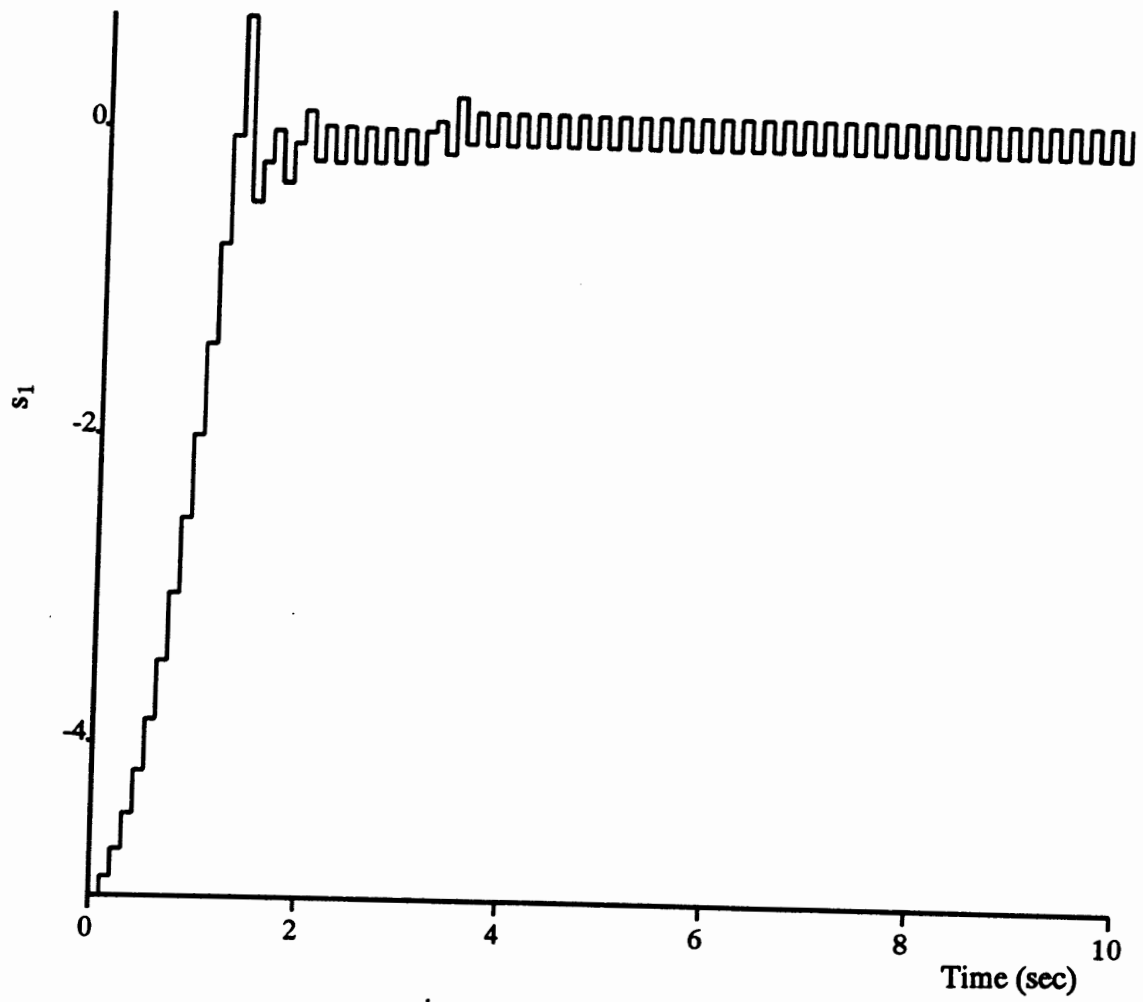
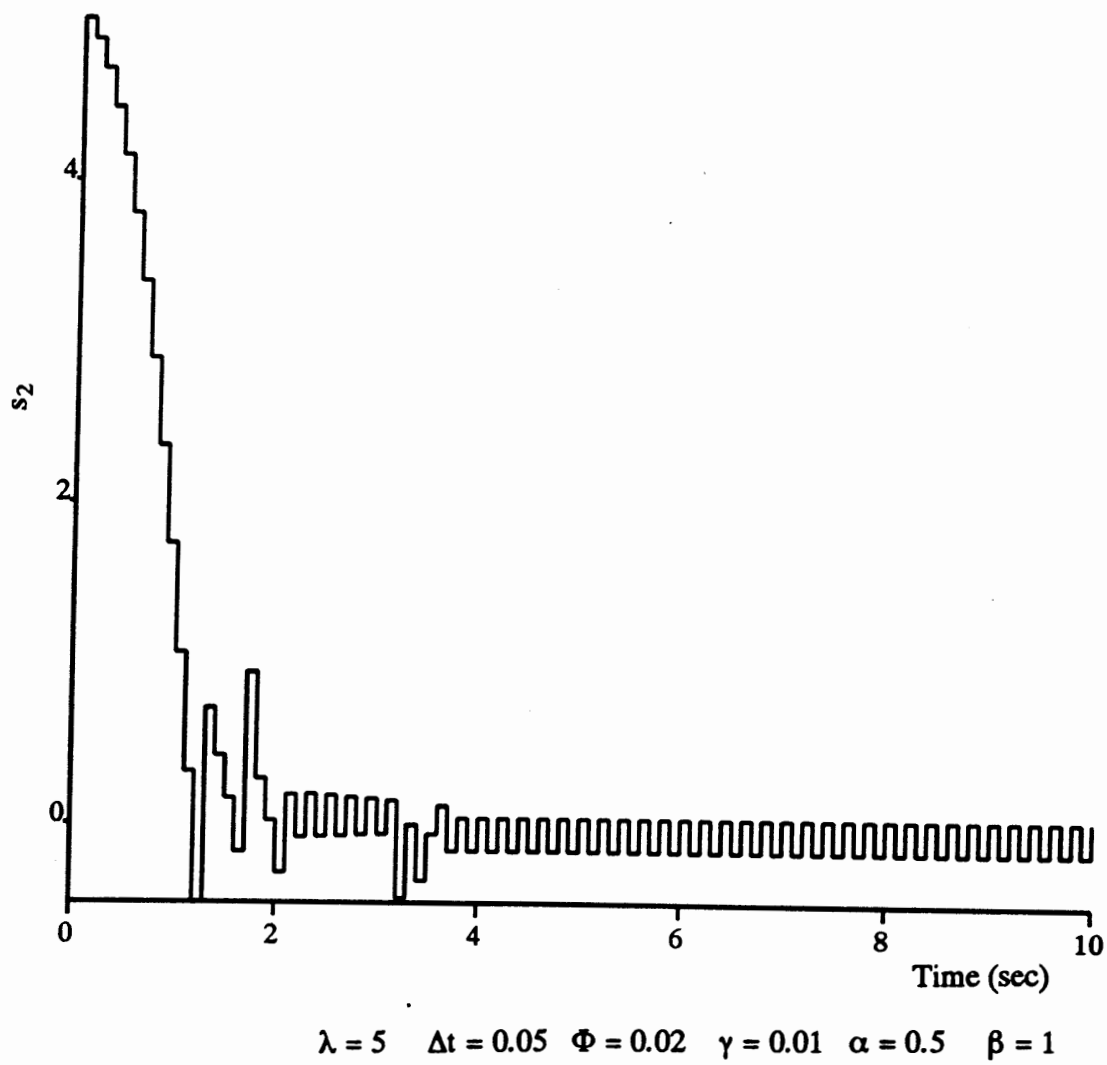


Figure 20. 2-nd Link Trajectory and Desired Trajectory



$$\lambda = 5 \quad \Delta t = 0.05 \quad \Phi = 0.02 \quad \gamma = 0.01 \quad \alpha = 0.5 \quad \beta = 1$$

Figure 21. $s_1(k)$

Figure 22. $s_2(k)$

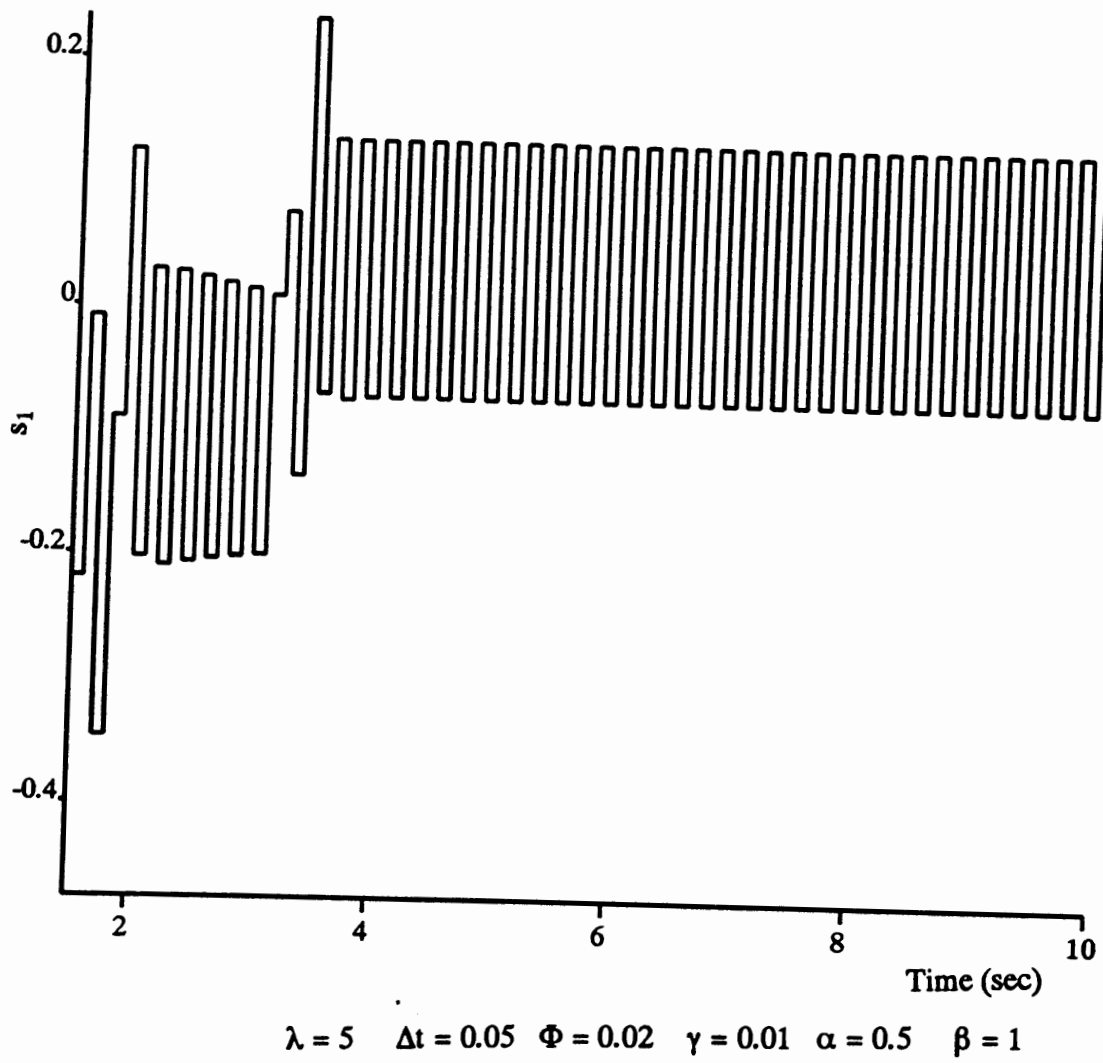
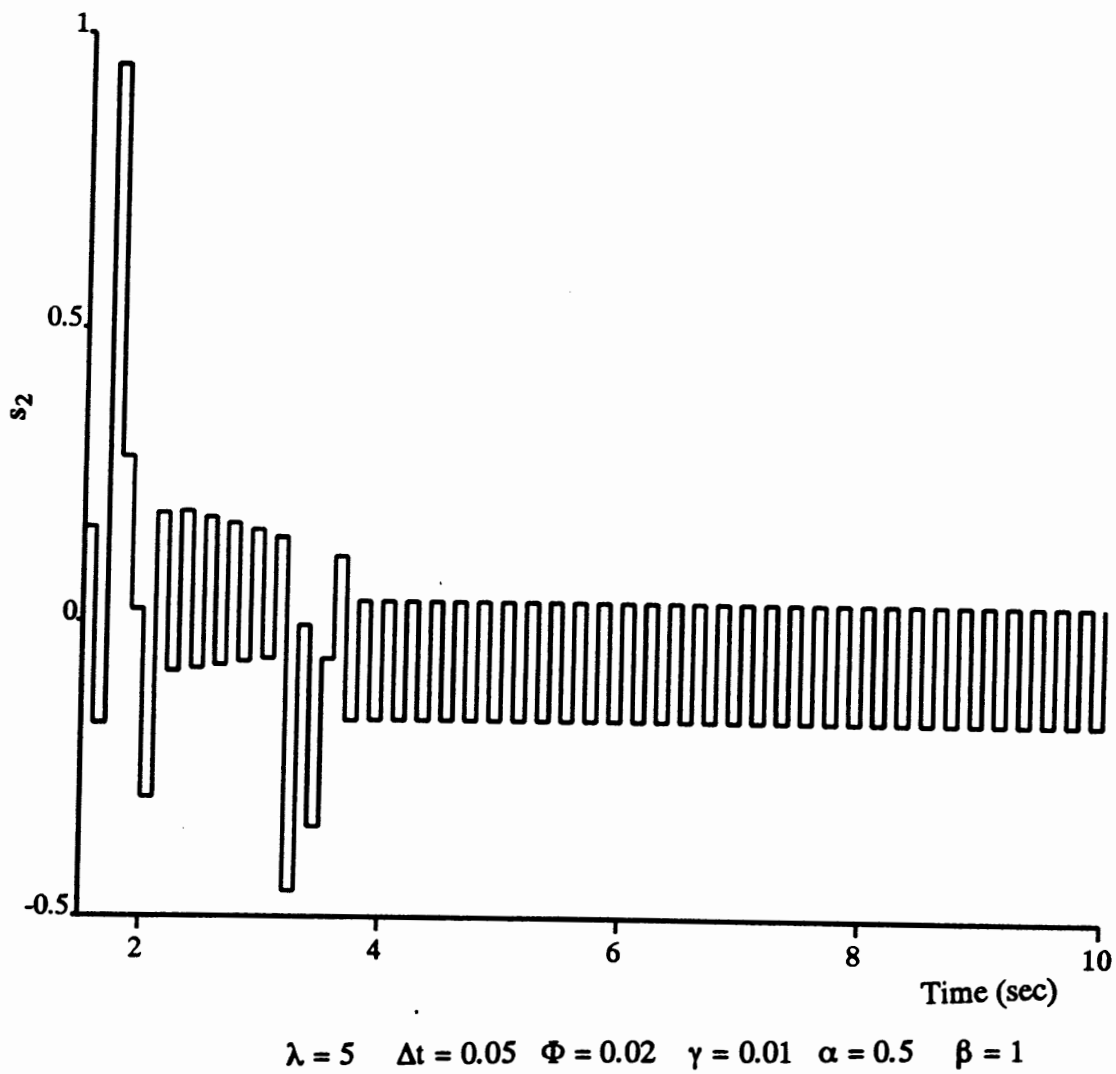


Figure 23. Zooming of $s_1(k)$

Figure 24. Zooming of $s_2(k)$

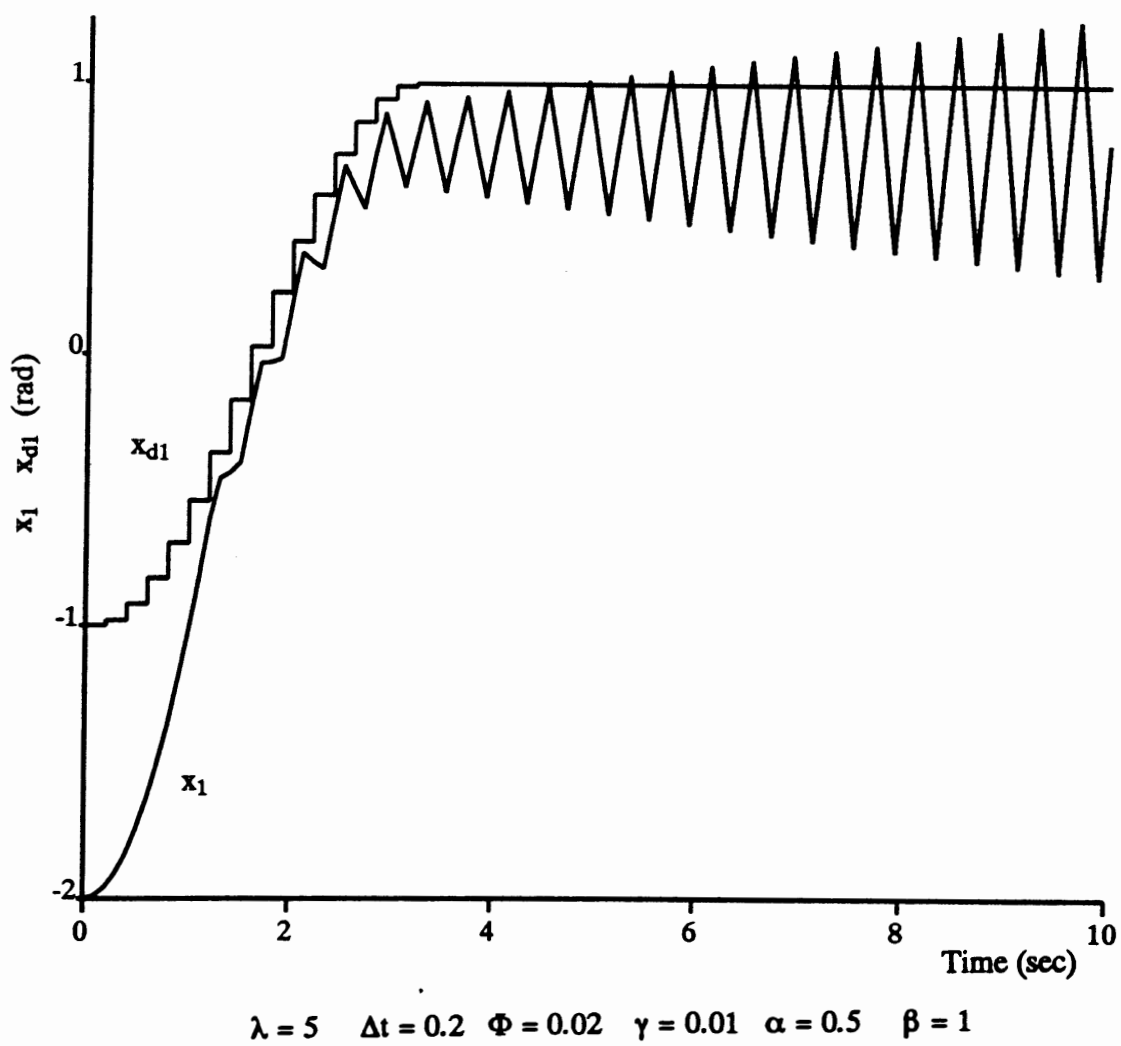


Figure 25 1-st Link Trajectory and Desired Trajectory

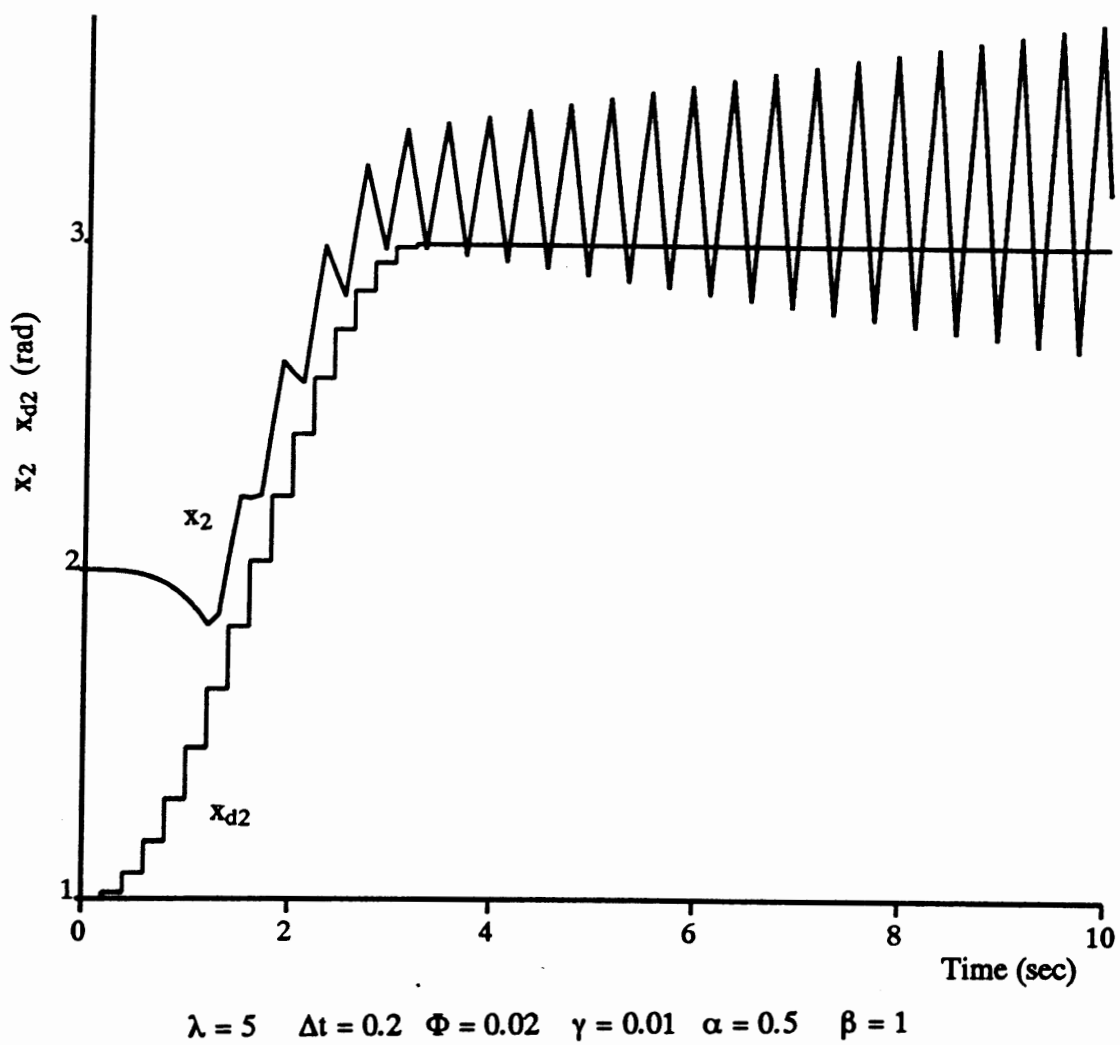
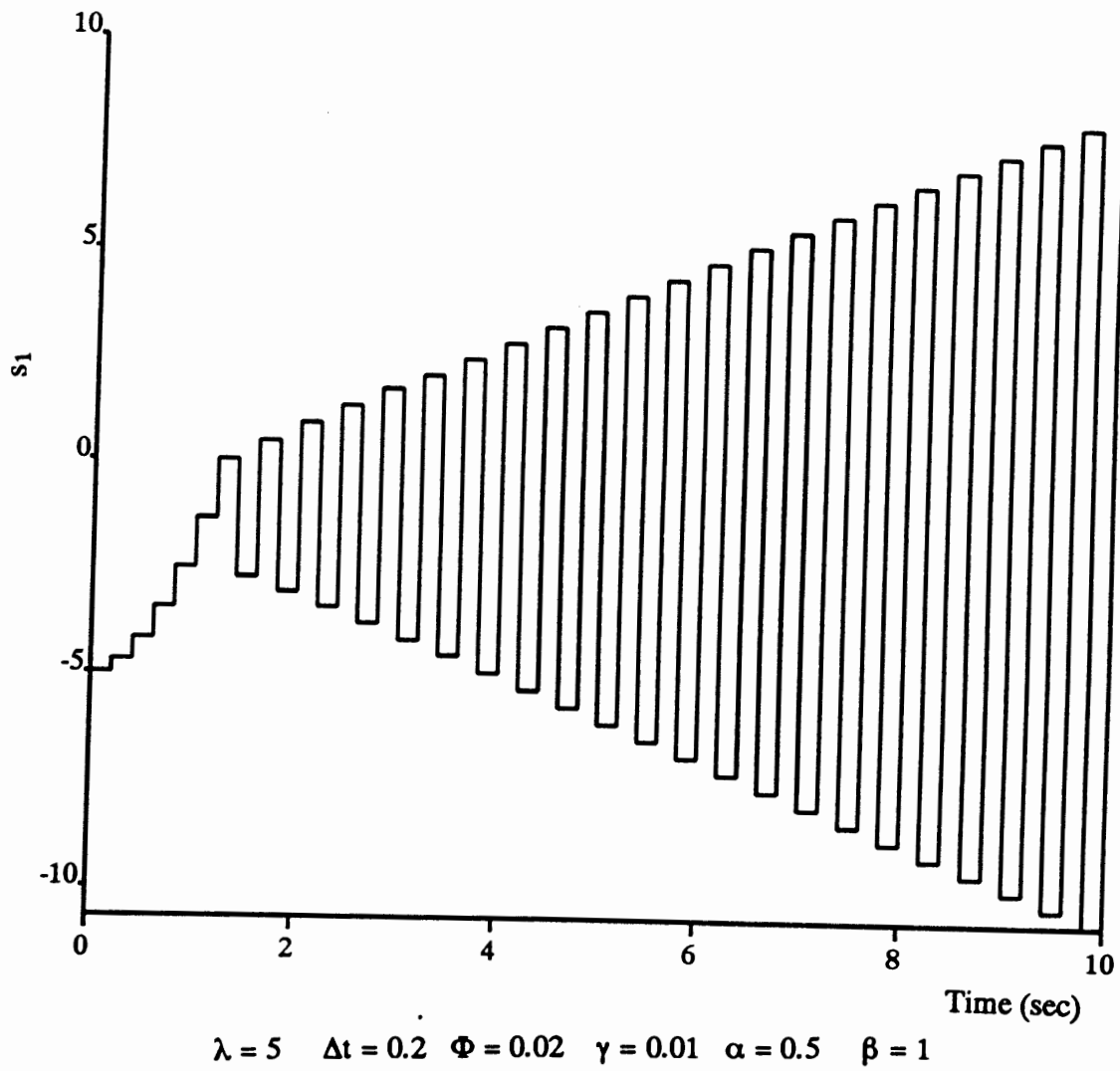
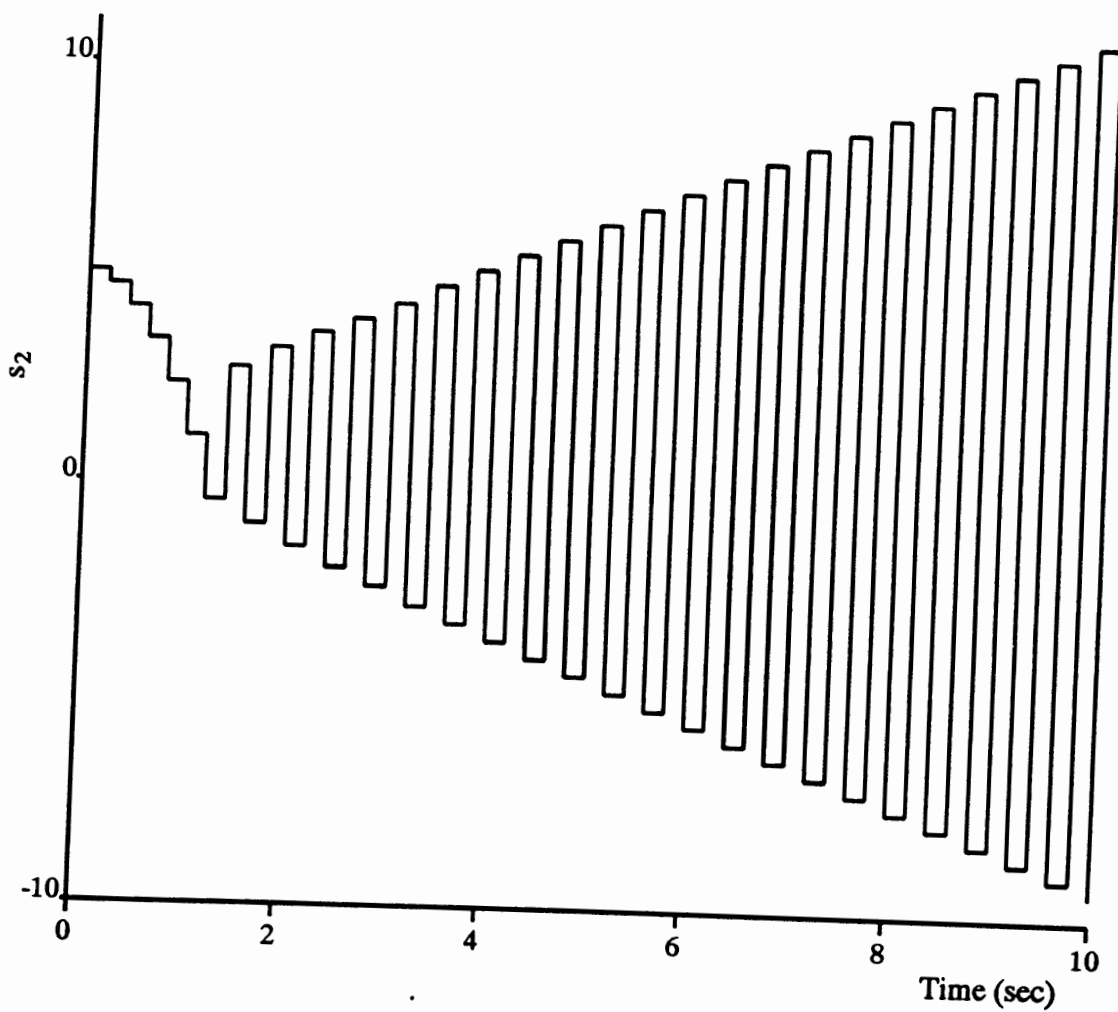


Figure 26. 2-nd Link Trajectory and Desired Trajectory

Figure 27. $s_1(k)$



$$\lambda = 5 \quad \Delta t = 0.2 \quad \Phi = 0.02 \quad \gamma = 0.01 \quad \alpha = 0.5 \quad \beta = 1$$

Figure 28. $s_2(k)$

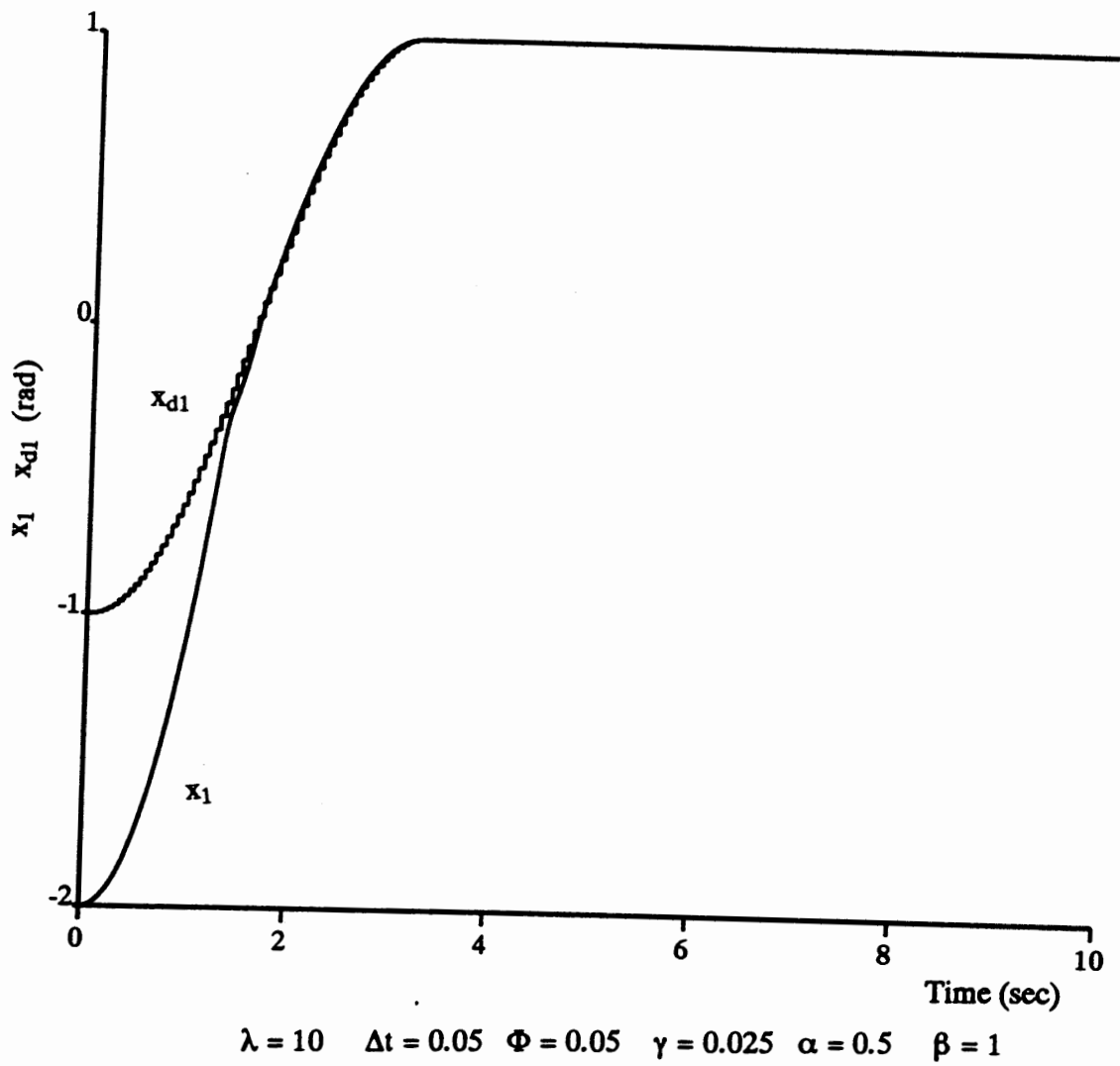
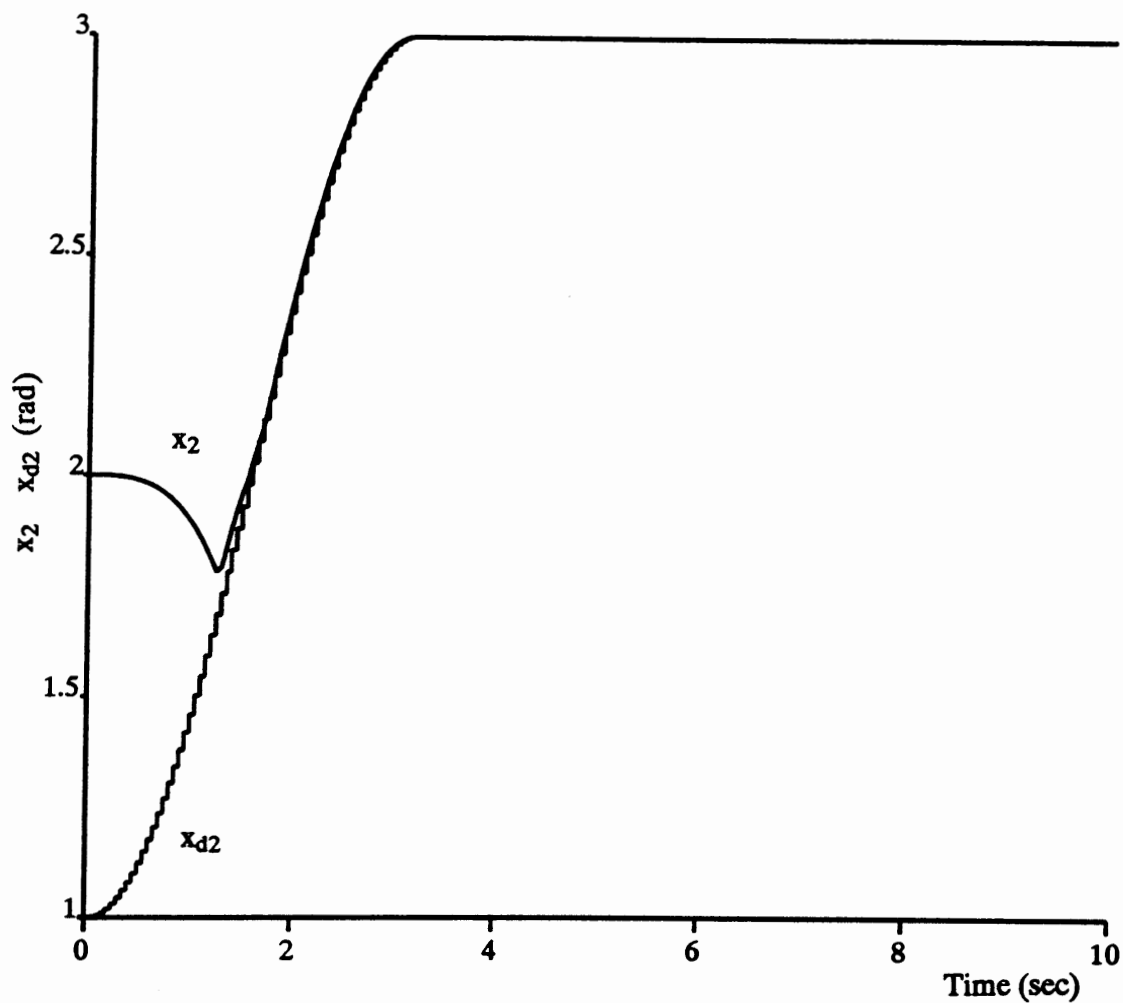
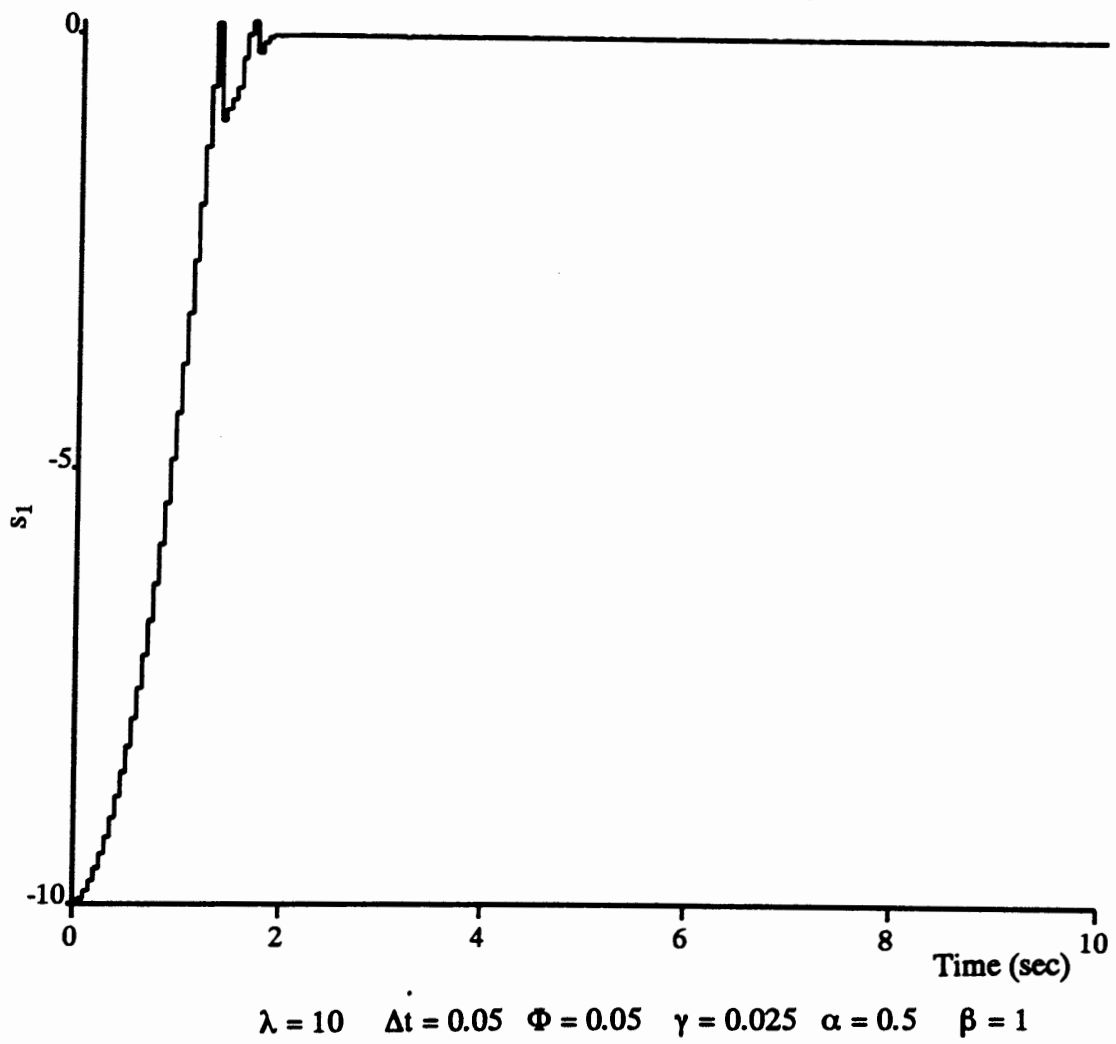


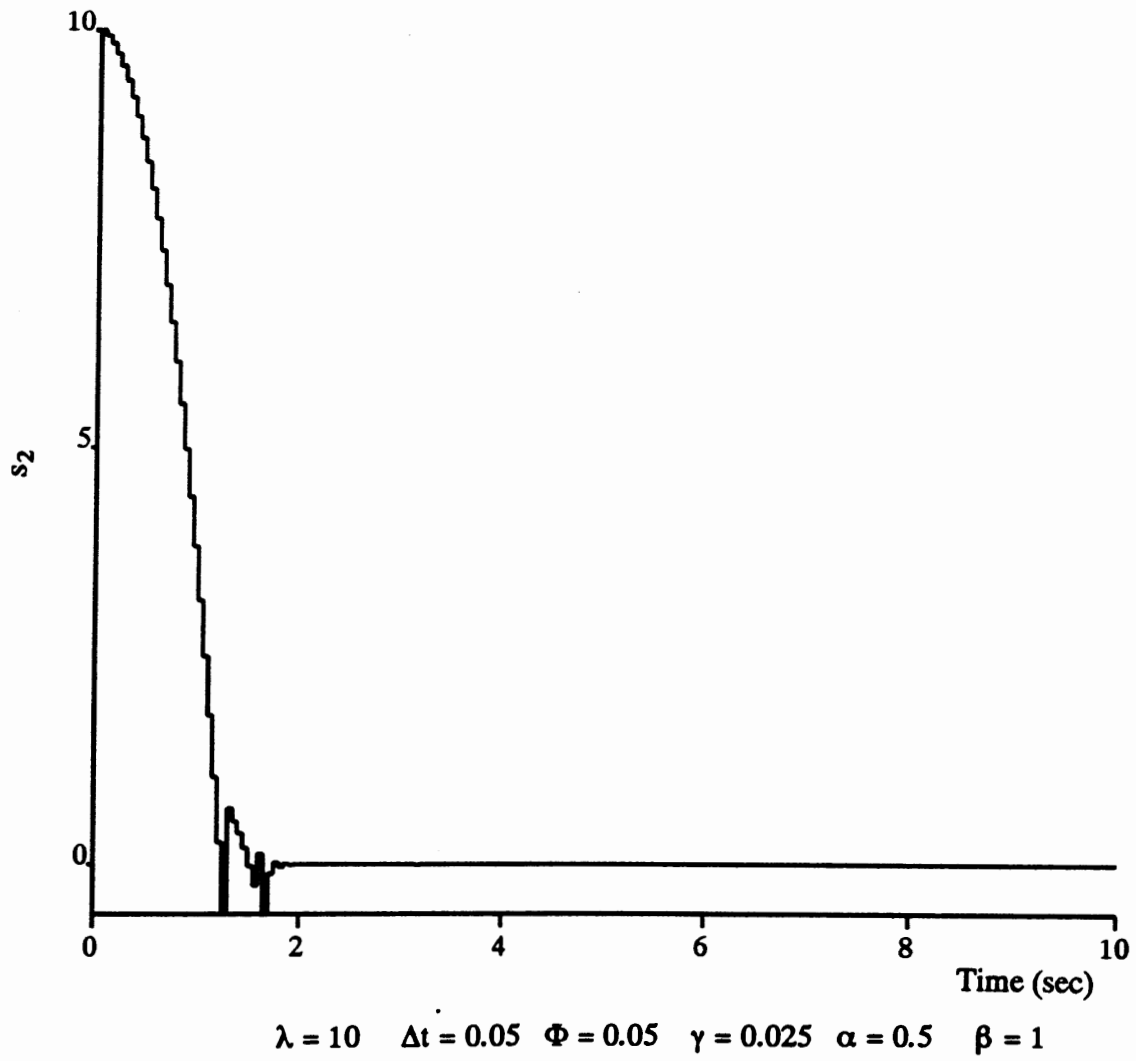
Figure 29. 1-st Link Trajectory and Desired Trajectory

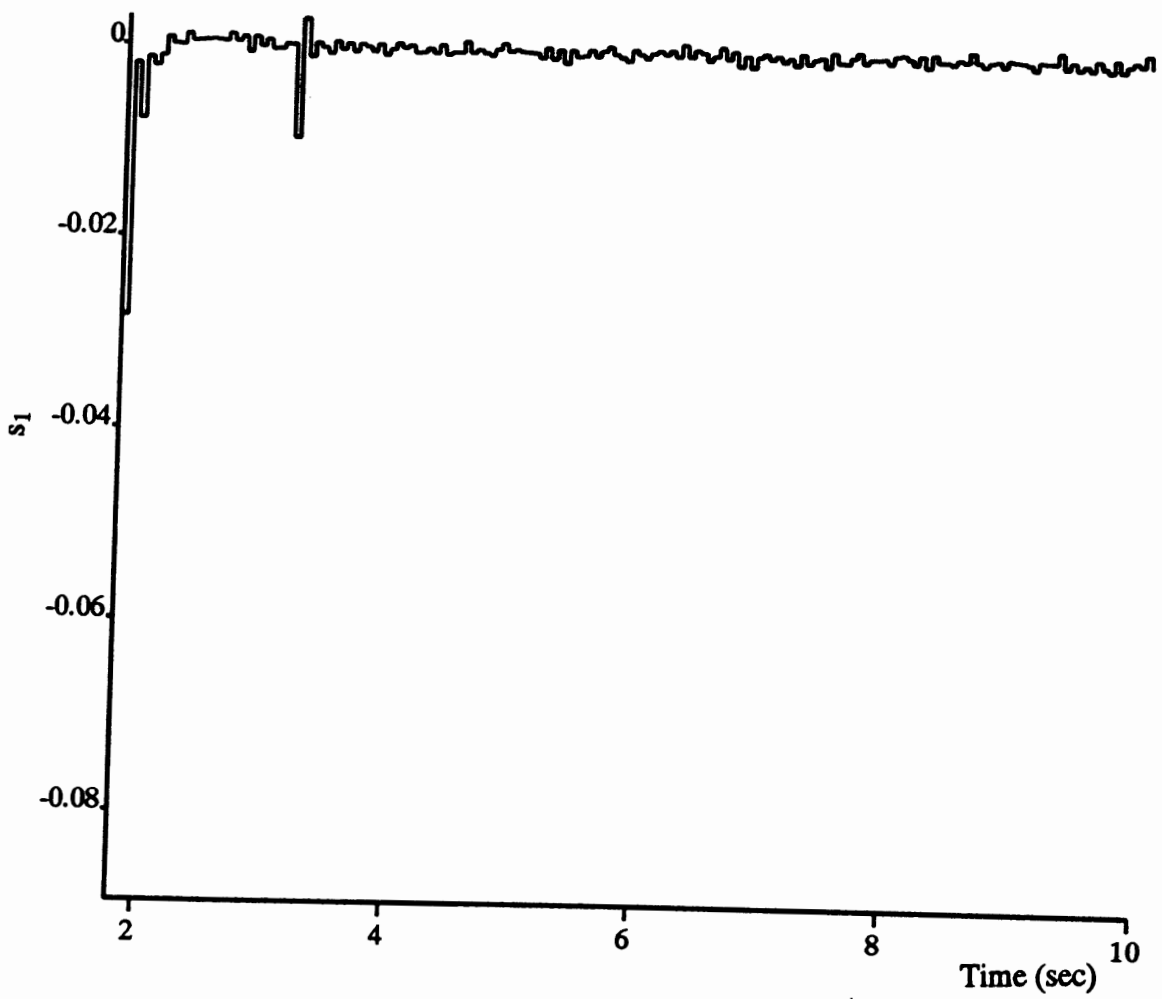


$$\lambda = 10 \quad \Delta t = 0.05 \quad \Phi = 0.05 \quad \gamma = 0.025 \quad \alpha = 0.5 \quad \beta = 1$$

Figure 30. 2-nd Link Trajectory and Desired Trajectory

Figure 31. $s_1(k)$

Figure 32. $s_2(k)$



$$\lambda = 10 \quad \Delta t = 0.05 \quad \Phi = 0.05 \quad \gamma = 0.025 \quad \alpha = 0.5 \quad \beta = 1$$

Figure 33. Zooming of $s_1(k)$

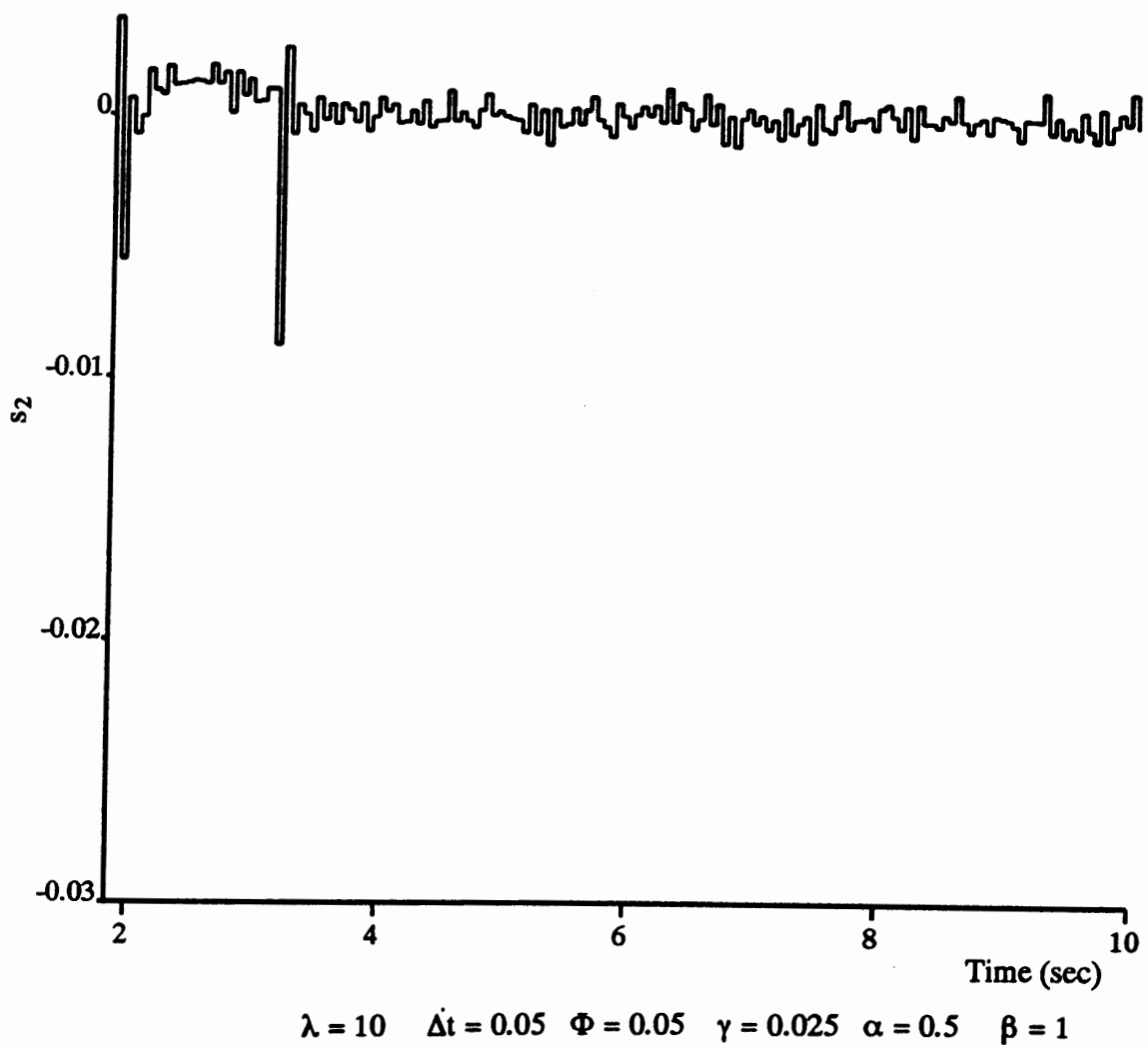
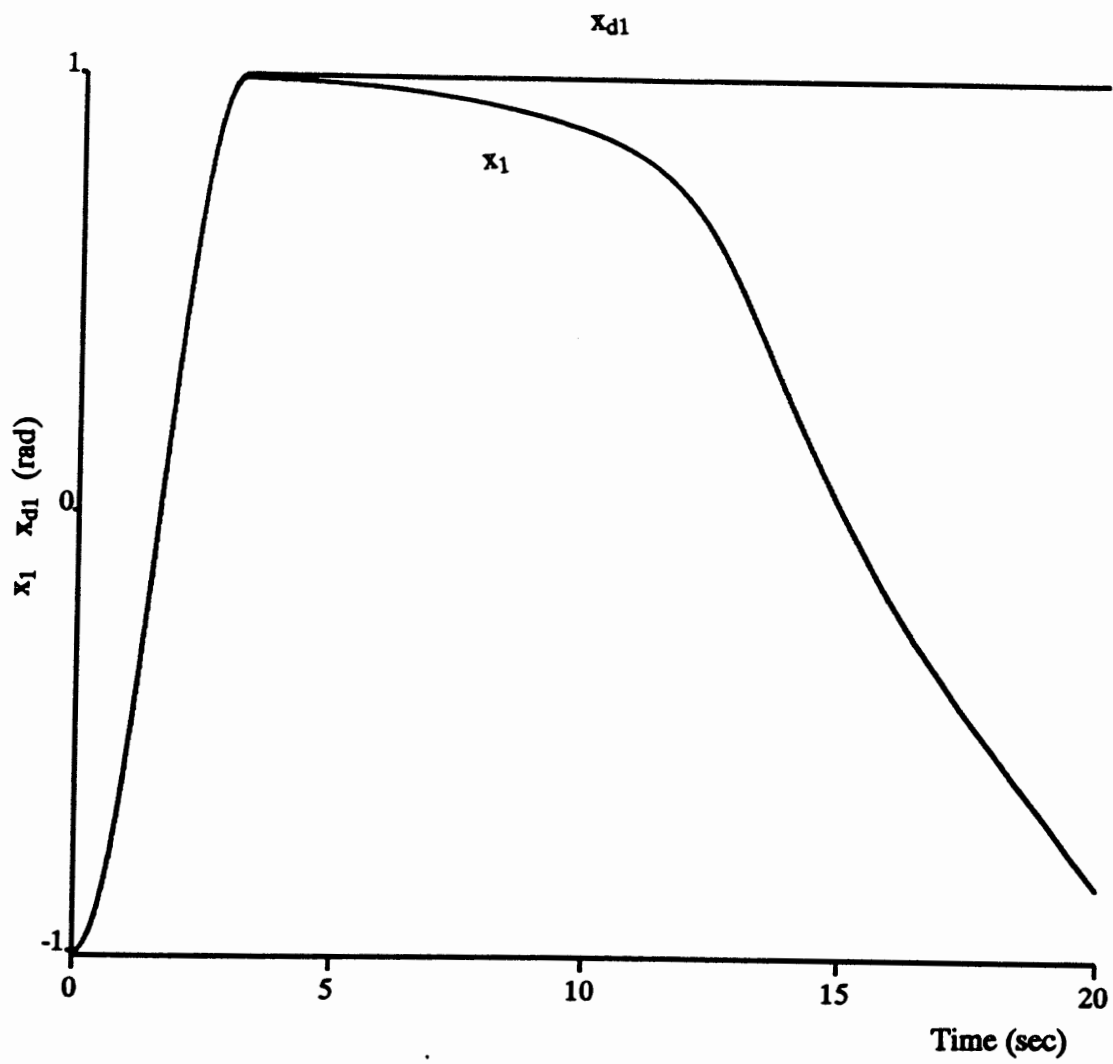
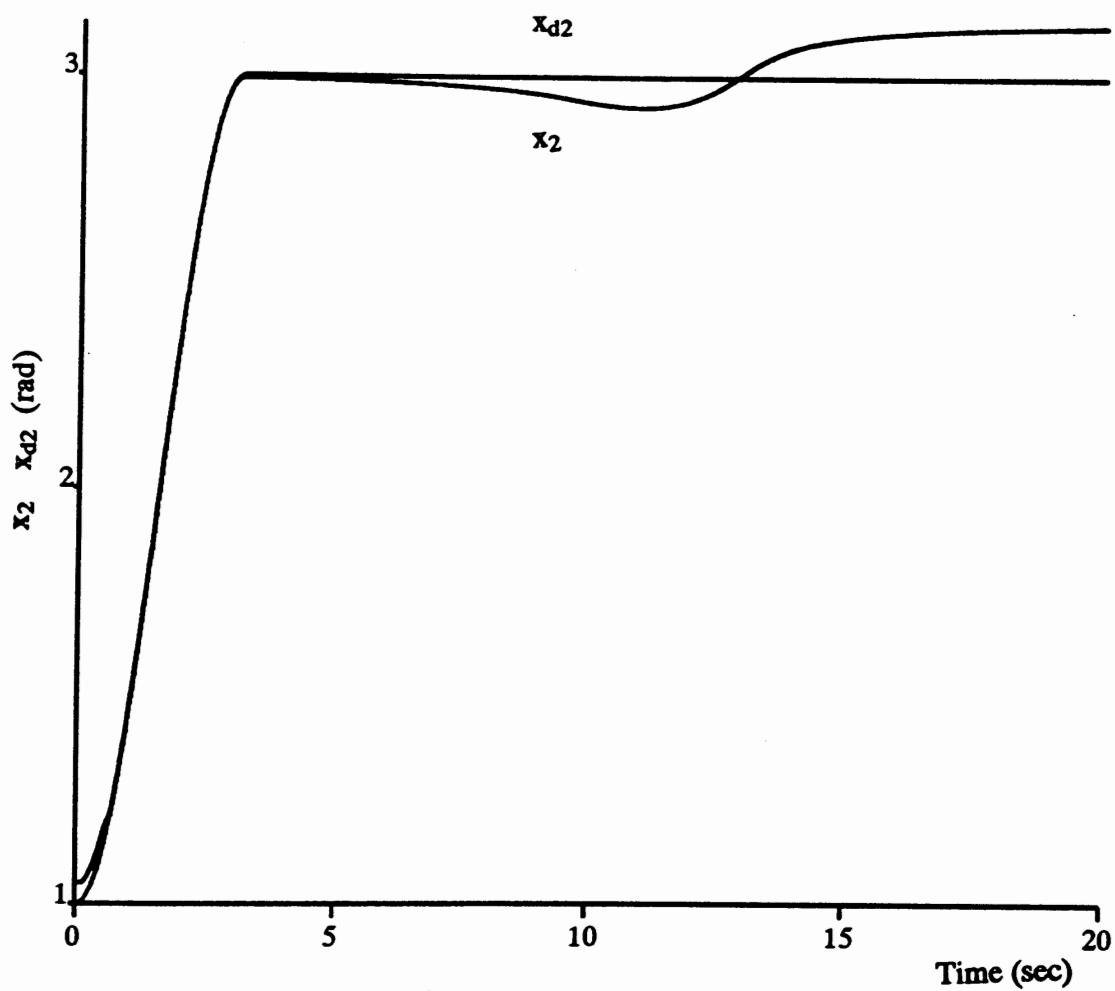


Figure 34. Zooming of $s_2(k)$



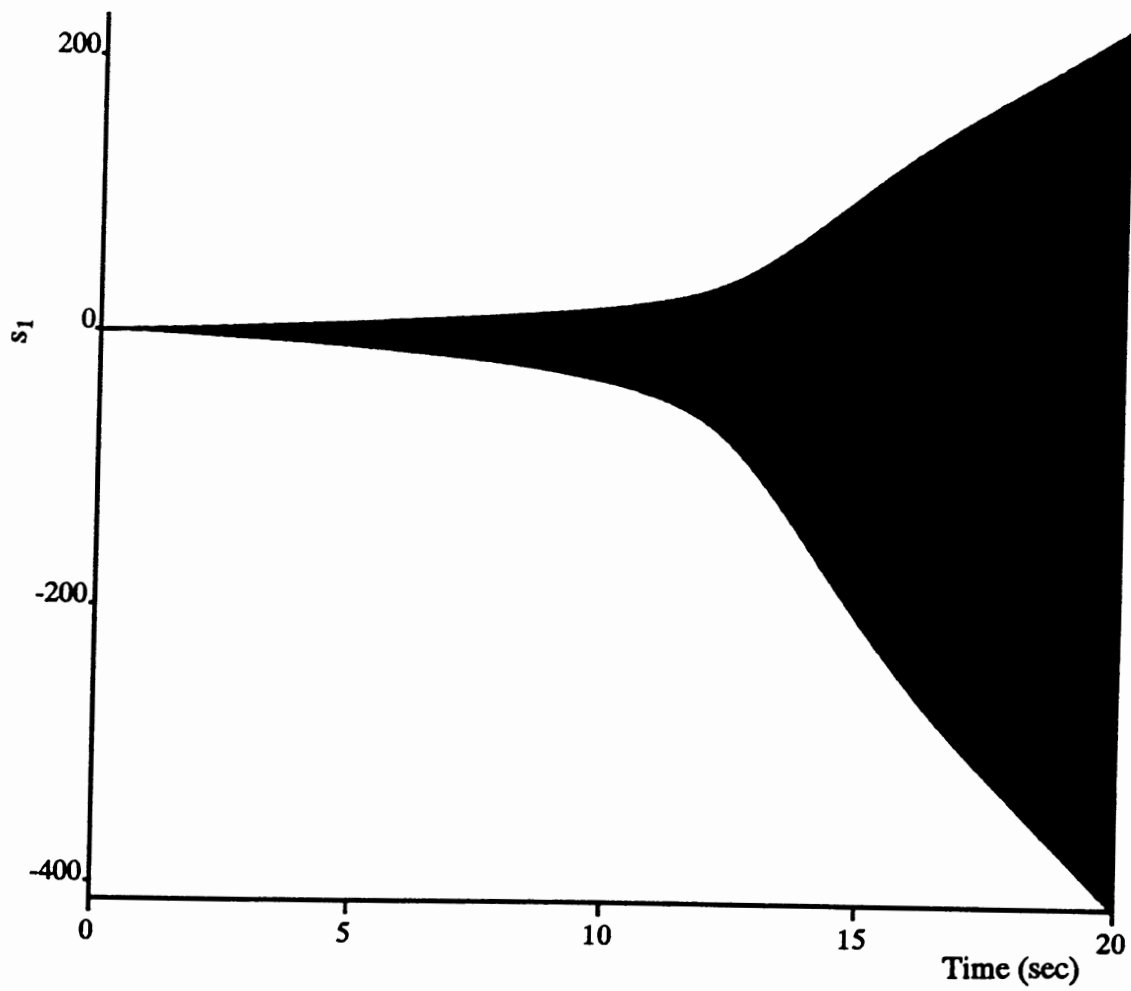
$$\lambda = 50 \quad \Delta t = 0.02 \quad \Phi = 0.05 \quad \gamma = 0.025 \quad \alpha = 0.5 \quad \beta = 1$$

Figure 35. 1-st Link Trajectory and Desired Trajectory



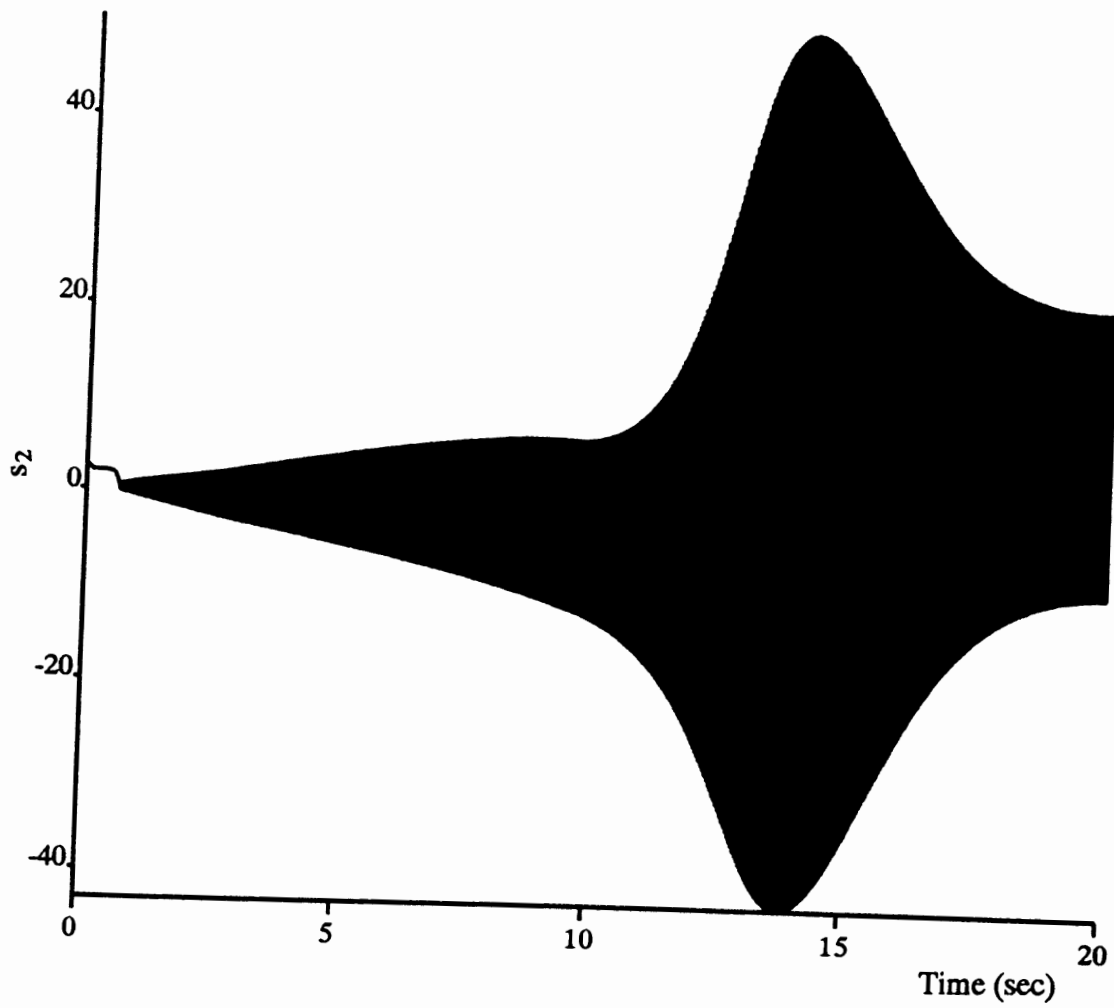
$$\lambda = 50 \quad \Delta t = 0.02 \quad \Phi = 0.05 \quad \gamma = 0.025 \quad \alpha = 0.5 \quad \beta = 1$$

Figure 36. 2-nd Link Trajectory and Desired Trajectory



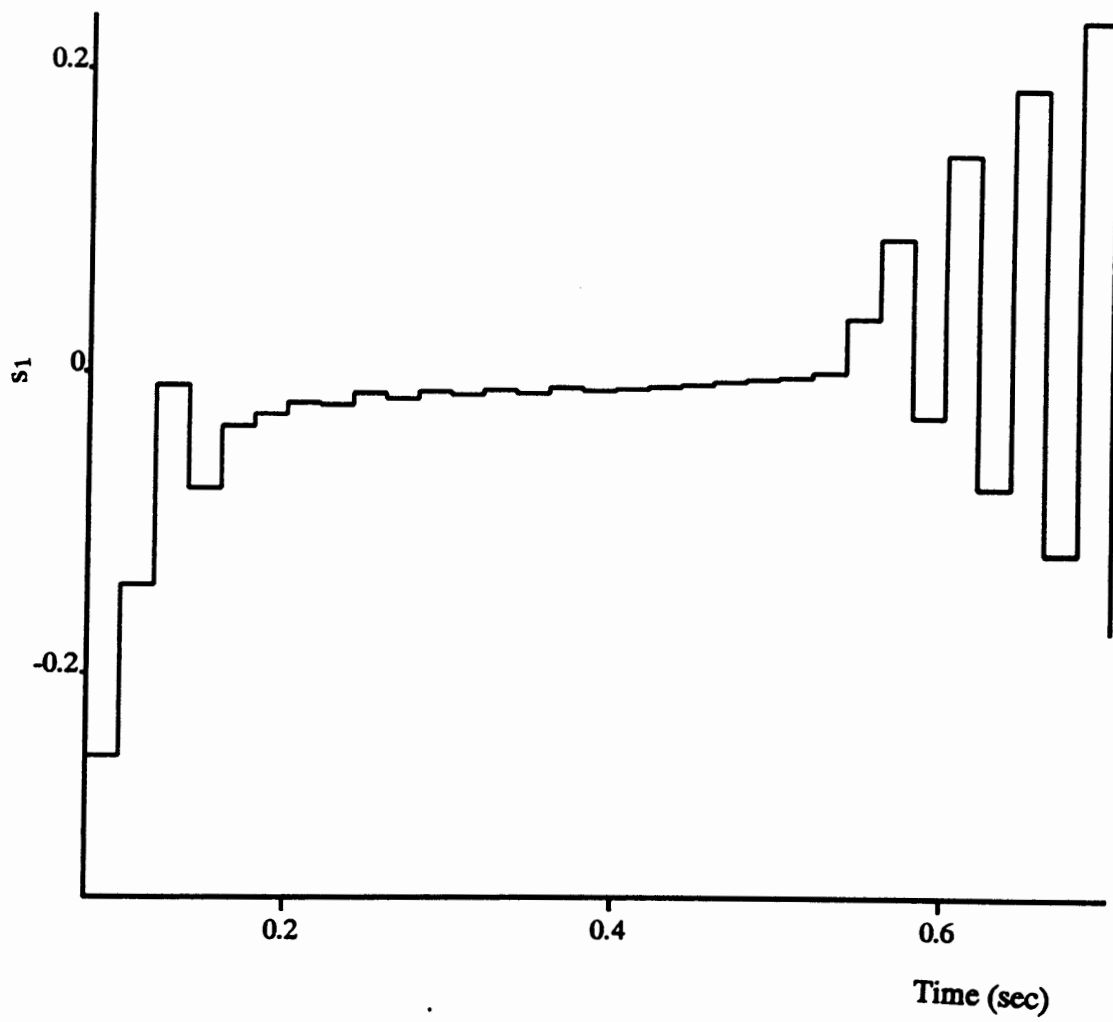
$$\lambda = 50 \quad \Delta t = 0.02 \quad \Phi = 0.05 \quad \gamma = 0.025 \quad \alpha = 0.5 \quad \beta = 1$$

Figure 37. $s_1(k)$



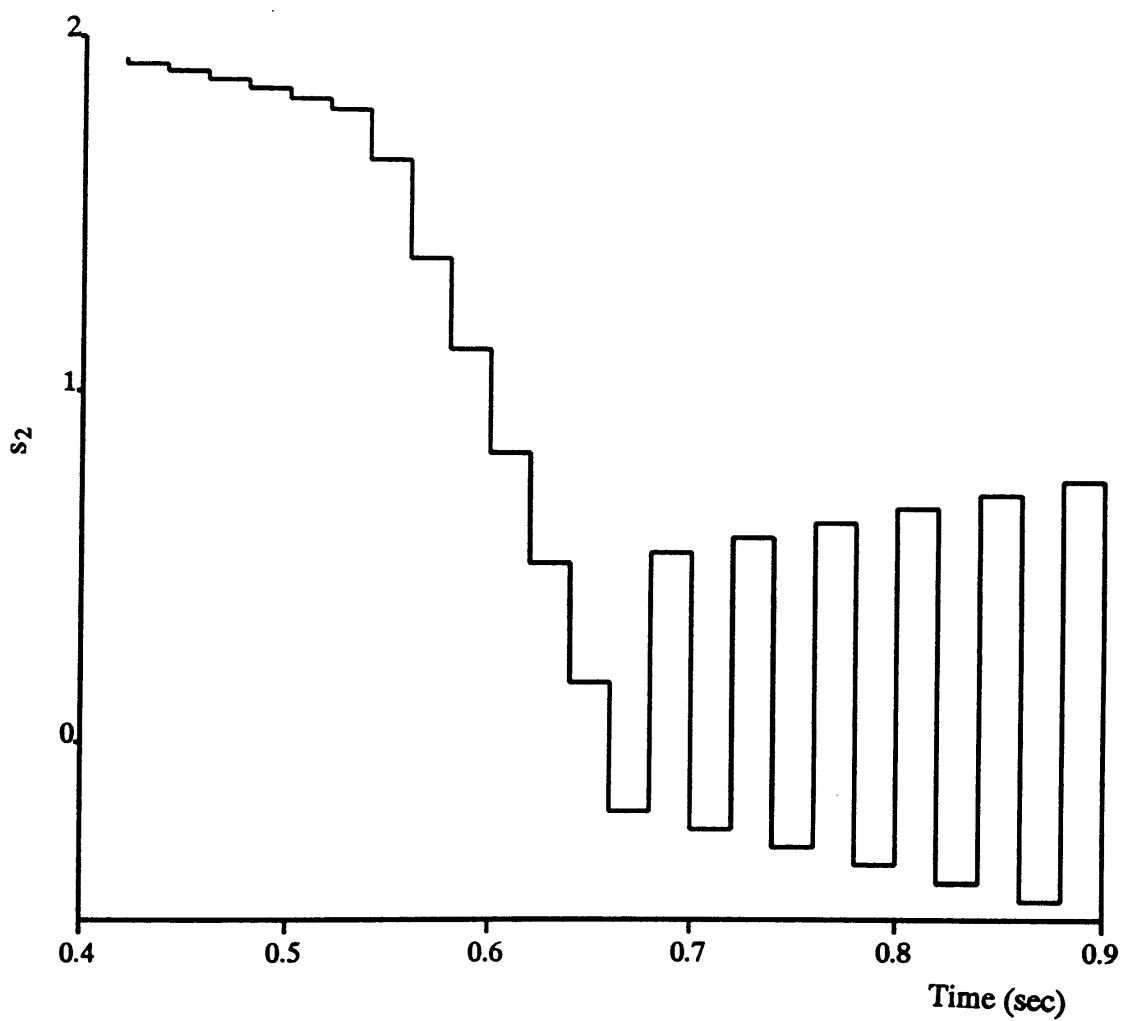
$$\lambda = 50 \quad \Delta t = 0.02 \quad \Phi = 0.05 \quad \gamma = 0.025 \quad \alpha = 0.5 \quad \beta = 1$$

Figure 38. $s_2(k)$



$$\lambda = 50 \quad \Delta t = 0.02 \quad \Phi = 0.05 \quad \gamma = 0.025 \quad \alpha = 0.5 \quad \beta = 1$$

Figure 39. Zooming of $s_1(k)$



$$\lambda = 50 \quad \Delta t = 0.02 \quad \Phi = 0.05 \quad \gamma = 0.025 \quad \alpha = 0.5 \quad \beta = 1$$

Figure 40. Zooming of $s_2(k)$

CHAPTER V

CONCLUSIONS AND RECOMMENDATIONS

Conclusions

This thesis focuses on the design parameters and design strategies for the system's stability of the discrete-time sliding mode control in the presence of modeling error. The overall objective was to establish a criterion for determining the sampling time of the sliding mode control used in a digital computer because the sampling will affect the stability of the system.

In the continuous domain, the sliding mode control uses a discontinuous switching function when the system trajectory crosses the sliding surface. In the discrete time domain, on the other hand, this study implements the square method to the sliding mode control in an effort to find out the changing rate of the trajectory. Also, we use this result to derive the control input and the thickness of the boundary layer, which should be greater than the modeling errors and disturbances.

Inside the boundary layer we use the saturation function in order to smooth the trajectory and to avoid invoking the unmodeled high frequency. However, the drawback of this smooth process is that it doesn't reach the desired point quickly. Some period of time is required for the convergence because the tracking error converges as a first order filter.

The sampling time and approaching rate have their limitations because they require stability consideration. Actually, the sliding mode control is a process of feedback linearization and it places new poles in desired places. The design parameters of the approaching rate and sampling time are factors that place the poles within the unit circle in the discrete time domain.

The advantage of the sliding mode control is that it is robust to the modeling error and noise. This research shows that the sliding mode control has the same ability in the discrete time domain. As long as the boundary layer thickness is larger than the upper bound of the modeling error and noise, the discrete time sliding mode control can be robust. In addition, the steady state trajectory error can be bounded in an acceptable value.

In summary, the research reported here has established a way to design the discrete-time sliding mode control in the presence of modeling error and noise. This methodology is verified in the analysis of stability. The use of this method will enable engineers to implement the sliding mode control to digital computers, and to determine a sampling time with high reliability.

Recommendations

While the discrete time sliding mode control has successfully simulated in the robot manipulators, the sliding mode algorithms can still be applied for use in the real world. Also, those control algorithms can be utilized in several different ways. This research explored a problem in determining the MIMO sliding surfaces. It offers new knowledge of great value regarding the design of the discrete-time controller. In order to promote further development of the technology, I suggest the following advanced researches

1. Used in an IBM 486 computer, the discrete sliding mode will demonstrate its ability to control a SCARA robot. The first thing to do is to identify the SCARA robot's parameters by using identification skills. The feedback signals contain noises which will prevent the proper parameter identification and endanger the control effort. Adding some filters in the feedback sensor, the controller could be run in a smoother manner.

2. MIMO sliding mode control can deal with high order degree of freedom system. However, the distances between the trajectories to sliding surfaces are difficult to figure out theoretically. Therefore, it is advisable that future studies focus on linear algebra to deal with coupling terms of the distance.

3. The sliding observer in the continuous domain is a new algorithm developed by some engineers. On the other hand, few researchers work on studies in discrete time domain. The stability analysis of the discrete sliding observer would be the next issue of this research.

4. Using square method to build up the membership function of Fuzzy Logic control, people can probably analyze the stability problem.

BIBLIOGRAPHY

1. Ambrosino, G., Celentano, G. and Garofalo. Variable structure model reference adaptive control systems. *Int J Control* 1984 v39, n6, p1339-1349.
2. Astrom K. J. and Wittenmark B.. *Adaptive control: Addison-Wesley* 1989.
3. Bose, B. K.. Sliding mode control of induction motor. *IEEE Conference record Industry Applications Society* 1985 v20, pp479-486.
4. Dote, Y. and Hoft, R. G.. Microprocessor based sliding mode controller for DC motor. *IEEE Industry Applications Society* 1980 v15, pp.641-645.
5. Dote, Y., Takebe, M. and Ito, T. .Variable structure control with sliding mode for DC drive speed regulation. *IEEE power electronics specialists conference* 1982, pp 123-127
6. Drakunov, S. V. and Utkin, V. I. . On discrete-time sliding modes, preprint of *IFAC Symposium*, June, 1989, p 14-16.
7. Egardt B.. *Stability of adaptive controllers. Lecture notes in control and information Sci*, 1979 v20, Berlin, Germany, Springer-Verlag.
8. Emilyanov S. V.. *Variable structure control system. Nanka: Moscow*, 1967.
9. Erschler J. and co-workers. Automation of Hydroelectric power station using variable-structure control system. *Automatica* 1974, 10, 31.
10. Espanc, M. D., Oretega, R. S. and Espino, J. J.. Variable structure systems with chattering reduction: a microprocessor based design. *Automatica* 1984 v20, n1, pp 133-134

11. Goodwin G. C. and Sin K. S.. Adaptive filtering, prediction and control : Prentice Hall 1984.
12. Habibi, S. R. and Richards, R. J.. Sliding mode control of an electrically powered industrial robot. IEE Proceedings 1992 v139, n2, pp207-225.
13. Hsu P. S., Sastry M., Bodson and Paden B.. Adaptive identification and control of manipulators without joint acceleration measurement, IEEE Int. conf. on Robotics and Automation, Raleigh, North Carolina.
14. Karunadasa, J. P. and Renfrew, A. C. . Design and implementation of microprocessor based sliding mode controller for brushless servomotor. IEE Proceedings, part B: Electric Power Applications 1991 v 138 n 6 p345-363.
15. Klein C. A. and Maney J. H. . Real-time control of manipulator-element mechanical linkage with a microcomputer. IEEE Trans. Ind. Elect. and Cont. Inst, IECEI-26,227.
16. Li, W. and Slotine, J. J.. Indirect adaptive robot control System control letter 12, 1988 p259-266.
17. Milosavljevic, C. . General conditions for the existence of a quasisliding mode on the switching hyperplane in discrete variable strycture systems. Automatica 1985 No.3, p 36-44.
18. Naik S. M., Kumar P. R. and Ydstie B. E.. Robust continuous-time adaptive control by parameter projection. IEEE Trans. on Aut. Control 1992 v37, n2.
19. Narendra K. S. and Annaswamy A. M.. Stable adaptive system: Prentice Hall 1989.
20. Park P. D.. Lyapunov redesign of model reference adaptive control systems. IEEE Trans. on Aut Control 1966 v11, p362.
21. Pieper, J. K. and Surgenor, B. W.. Optimal sliding surface design for discrete time sliding mode control. to be published.

22. Sarpturk, S. Z., Istefanopulos, Y. and Kaynak, O.. On the stability of discrete-time sliding mode control system. *IEEE Trans. on Aut. Control* 1989 v. AC-32, No.10,
23. Slotine J. J. and Coetsee J. A.. Adaptive Sliding controller synthesis for nonlinear systems. *Int. J. Control* 1986.
24. Slotine J. J. and Li, W. . *Applied nonlinear control*: Prentice Hall, 1991.
25. Slotine J. J. and Li, W.. Composite adaptive control of robot manipulator, *Automatica*1989 25, 4.
26. Slotine J. J. and SastryS. S.. Tracking control of non-linear systems using sliding surface, with application to robot manipulators. *Int. J. Control* 1983 v38, n2, PP465-492.
27. Slotine, J. J.and Li, W. . On the adaptive control of robot manipulators. *Int. J. Robotics Res.*1987, 6, 3.
28. Spurgeon, S. K. . On the development of discrete-time sliding mode control systems. *International conference on control '90 25-28 March 1991 pp. 505-510.*
29. Tsakalis K. S.. Robustness of model reference adaptive controllers: an input-output approach. *IEEE Trans. on Aut. Control* 1992 v37, n5.
30. Utkin V. L. Variable structure systems with sliding modes. *IEEE Trans. Aut. Control* 1977, AC-22,211.
31. Wen J. T., Krentz-Delgado K. K. and Bayard D. S.. Lyapunov function-based control law for revolute robot arms: Tracking control robustness and adaptive control. *IEEE Trans. Aut. Control* 1992 v37, n2.
32. Wit, C. C. and Astrom, K. J.. Trajectory tracking in robot manipulators via nonlinear estimated state feedback. *IEEE Trans. on Robotics and Automation* 1992 v8, n1.
33. Young, G. E. and Rao, S.. Robust sliding-mode control of a nonlinear process with uncertainty and delay. *Journal of dynamic systems, measurement, and control* 1987 v109, p.203-208.

APPENDIX

**MODEL DESCRIPTION OF THE SCARA ROBOT ROBOT
AND DYNAMIC EQUATION DERIVED**

MODEL DESCRIPTION

Introduction

We are analyzing the relationship between the actuator torque and joint angular acceleration for a device with two degrees of freedom, such as arm on a lathe machine. The method presented here utilizes the Euler-Lagrange equation. We use this method to provide a clear understanding of the effect of varying inertia, joint interaction, and coriolis force. It also forms the basis of simulation of such a system and, most importantly, design of control system.

Two-link Robot Model

A two-degree-of-freedom robot arm manipulator with is equipped at each joint with an actuator DC motor to provide input torque, an encoder for measuring joint position , and a tachometer for measuring joint velocity. Fig 10 shows the outlook of the system.

Here we assume the concentrate-masses locate at the distance of l_1 , l_2 with respect to joint O and A, respectively.

- * l_1 : distance of 1st link center of mass to joint O
- * l_2 : distance of 2nd link center of mass to joint A

- * L1: length of 1st link
 - * L2: length of 2nd link
 - * m1: concentrate-mass of 1st link
 - * m2: concentrate-mass of 2nd link
 - * j1: total moment of inertia of 1st link
 - * j2: total moment of inertia of 2nd link
 - * θ_1 : angular displacement of 1st link about to vertical line
 - * θ_2 : angular displacement of 2nd link about 1st link
- The angular velocity of 1st and 2nd link is $\dot{\theta}_1$ and $\dot{\theta}_2$ respectively.

Dynamic equation Derivation

The easiest technique is based on the Euler-Lagrange Formula:

$$\Gamma_i = \frac{d}{dt} \left(\frac{\partial L}{\partial \dot{\theta}_i} \right) - \frac{\partial L}{\partial \theta_i}$$

where

Γ_i : actuators torque apply to the i^{th} joint

L : mechanical energy

$$L = K - V$$

where

K : kinetic energy of each link

V : potential energy

Kinetic energy

For link 1

$$\vec{V}_1 = \dot{\theta}_1 \vec{r}_1 \times \vec{l}_1$$

$$K_1 = \frac{M_1 V_1^2}{2} + \frac{J_1 \dot{\theta}_1^2}{2}$$

$$= \frac{1}{2} (J_1 + m_1 l_1^2) \dot{\theta}_1^2$$

For link 2

$$\vec{V}_2 = \vec{V}_a + (\dot{\theta}_1 + \dot{\theta}_2) \vec{l}_2$$

$$= [\dot{\theta}_1 L_1 \cos \theta_1 + (\dot{\theta}_1 + \dot{\theta}_2) l_2 \cos (\theta_1 + \theta_2)] \hat{i}$$

$$+ [\dot{\theta}_1 L_1 \sin \theta_1 + (\dot{\theta}_1 + \dot{\theta}_2) l_2 \sin (\theta_1 + \theta_2)] \hat{j}$$

$$\vec{V}_2^2 = \dot{\theta}_1^2 L_1^2 + (\dot{\theta}_1 + \dot{\theta}_2)^2 l_2^2 + 2L_1 l_2 \dot{\theta}_1 (\dot{\theta}_1 + \dot{\theta}_2) \cos (\theta_1 - \theta_1 - \theta_2)$$

$$= \dot{\theta}_1^2 L_1^2 + (\dot{\theta}_1 + \dot{\theta}_2)^2 l_2^2 + 2L_1 l_2 \dot{\theta}_1 (\dot{\theta}_1 + \dot{\theta}_2) \cos \theta_2$$

$$K_2 = \frac{1}{2} M_2 V_2^2 + \frac{1}{2} J_2 (\dot{\theta}_1 + \dot{\theta}_2)^2$$

$$K_2 = \left[\frac{1}{2} M_2 (L_1^2 + l_2^2 + 2L_1 l_2 \cos \theta_2) + \frac{1}{2} J_2 \right] \dot{\theta}_1^2 +$$

$$\left[\frac{M_2}{2} l_2^2 + \frac{1}{2} J_2 \right] \dot{\theta}_2^2 + [M_2 (L_1 l_2 \cos \theta_2) + J_2] \dot{\theta}_1 \dot{\theta}_2$$

$$K = K_1 + K_2$$

$$= \left[\frac{1}{2} (J_1 + J_2) + \frac{1}{2} M_1 l_1^2 + \frac{1}{2} M_2 (L_1^2 + l_2^2 + 2L_1 l_2 \cos \theta_2) \right] \dot{\theta}_1^2 +$$

$$\left[\frac{1}{2} M_2 l_2^2 + \frac{1}{2} J_2 \right] \dot{\theta}_2^2 + [M_2(l_2^2 + L_1 l_2 \cos \theta_2) + J_2] \dot{\theta}_1 \dot{\theta}_2$$

For the temporary requirement, we add the gravity force in the Y direction and treat it like a vertical double-pendulum. Then we consider the gravity force. The potential energy will be

Potential energy

$$V_1 = -M_1 g l \cos \theta_1$$

$$V_2 = -M_2 g (L_1 \cos \theta_1 + l_2 \cos (\theta_1 + \theta_2))$$

Total potential energy equals the energy summation of each link's potential energy.

$$V = V_1 + V_2$$

$$V = V_1 + V_2 = -g(M_1 l_2 + M_2 L_1) \cos \theta_1 - M_2 g l_2 \cos (\theta_1 + \theta_2)$$

Therefore, the total energy is

$$L = K - V = \left[\frac{1}{2} (J_1 + J_2) + \frac{1}{2} M_1 l_1^2 + \frac{M_2}{2} (L_1^2 + l_2^2 + 2L_1 l_2 \cos \theta_2) \right] \dot{\theta}_1^2$$

$$+ \left[\frac{1}{2} M_2 l_2^2 + \frac{1}{2} J_2 \right] \dot{\theta}_2^2 + [M_2(l_2^2 + L_1 l_2 \cos \theta_2) + J_2] \dot{\theta}_1 \dot{\theta}_2$$

$$+ g(M_1 l_1 + M_2 l_1) \cos \theta_1 + g M_2 l_2 \cos (\theta_1 + \theta_2)$$

Euler-Lagrangian rule

$$\frac{d}{dt} \left(\frac{\partial L}{\partial \dot{\theta}_1} \right) - \frac{\partial L}{\partial \theta_1} = \Gamma_1$$

$$\frac{\partial L}{\partial \dot{\theta}_1} = [J_1 + J_2 + M_1 l_1^2 + M_2 (L_1^2 + l_2^2 + 2L_1 l_2 \cos \theta_2)] \dot{\theta}_1$$

$$+ [M_2 (l_2 + L_1 l_2 \cos \theta_2) + J_2] \dot{\theta}_2$$

$$\begin{aligned} \frac{d}{dt} \left(\frac{\partial L}{\partial \dot{\theta}_1} \right) &= [J_1 + J_2 + M_1 l_1^2 + M_2 (L_1^2 + l_2^2 + 2L_1 l_2 \cos \theta_2)] \ddot{\theta}_1 \\ &\quad - (2M_2 L_1 l_2 \sin \theta_2) \dot{\theta}_2 \dot{\theta}_1 + [M_2 (l_2^2 + L_1 l_2 \cos \theta_2) + J_2] \ddot{\theta}_2 \\ &\quad - (M_2 L_1 l_2 \sin \theta_2) \dot{\theta}_2^2 \end{aligned}$$

$$\frac{\partial L}{\partial \theta_1} = -g(M_1 l_1 + M_2 L_1) \sin \theta_1 - g(M_2 l_2 \sin (\theta_1 + \theta_2))$$

$$\begin{aligned} \Rightarrow \Gamma_1 &= [J_1 + J_2 + M_1 l_1^2 + M_2 (L_1^2 + l_2^2 + 2L_1 l_2 \cos \theta_2)] \ddot{\theta}_1 \\ &\quad + [M_2 (l_2^2 + L_1 l_2 \cos \theta_2) + J_2] \ddot{\theta}_2 - (M_2 L_1 l_2 \sin \theta_2) (2\dot{\theta}_1 \dot{\theta}_2 + \dot{\theta}_2^2) \\ &\quad + g(M_1 l_1 + M_2 L_1) \sin \theta_1 + g[M_2 l_2 \sin (\theta_1 + \theta_2)] \end{aligned}$$

For link 2

$$\frac{d}{dt} \left(\frac{\partial L}{\partial \dot{\theta}_2} \right) - \frac{\partial L}{\partial \theta_2} = \Gamma_2$$

$$\frac{\partial L}{\partial \dot{\theta}_2} = (M_2 l_2^2 + J_2) \dot{\theta}_2 + [M_2 (l_2^2 + L_1 l_2 \cos \theta_2) + J_2] \dot{\theta}_2$$

$$\frac{d}{dt} \left(\frac{\partial L}{\partial \dot{\theta}_2} \right) = (M_2 l_2^2 + J_2) \ddot{\theta}_2 + [M_2 (l_2^2 + L_1 l_2 \cos \theta_2) + J_2] \ddot{\theta}_1$$

$$- [M_2 L_1 l_2 \sin \theta_2] \dot{\theta}_1 \dot{\theta}_2$$

$$\frac{\partial L}{\partial \theta_2} = -M_2 L_1 l_2 \sin \theta_2 \dot{\theta}_1^2 - (M_2 L_1 l_2 \sin \theta_2) \dot{\theta}_1 \dot{\theta}_2$$

$$- g M_2 l_2 \sin (\theta_1 + \theta_2)$$

$$\Gamma_2 = (M_2 l_2^2 + J_2) \ddot{\theta}_2 + [M_2 (l_2^2 + L_1 l_2 \cos \theta_2) + J_2] \ddot{\theta}_1$$

$$+ [M_2 L_1 l_2 \sin \theta_2] \dot{\theta}_1^2 + g M_2 l_2 \sin (\theta_1 + \theta_2)$$

To sum up, those term in matrix form

$$\mathbf{J}(\theta) \ddot{\theta} + \mathbf{C}(\theta, \dot{\theta}) \dot{\theta} + \mathbf{g}(\theta) = \Gamma$$

where

$$\mathbf{J}(\theta) = \begin{bmatrix} J_{11} & J_{12} \\ J_{21} & J_{22} \end{bmatrix}$$

$$J_{11} = J_1 + J_2 + M_1 l_1^2 + M_2 (L_1^2 + l_2^2 + 2L_1 l_2 \cos \theta_2)$$

$$J_{12} = M_2 (l_2^2 + L_1 l_2 \cos \theta_2) + J_2$$

$$J_{21} = M_2 (l_2^2 + L_1 l_2 \cos \theta_2) + J_2$$

$$J_{22} = M_2 l_2^2 + J_2$$

$$\mathbf{C}(\theta, \dot{\theta}) = \begin{bmatrix} -2M_2 L_1 l_2 \sin \theta_2 \dot{\theta}_2 & -2M_2 L_1 l_2 \sin \theta_2 \dot{\theta}_2 \\ M_2 L_1 l_2 \sin \theta_2 \dot{\theta}_1 & 0 \end{bmatrix}$$

$$\mathbf{g}(\boldsymbol{\theta}) = \begin{bmatrix} \mathbf{g}(M_1 l_1 + M_2 l_1) \sin \theta_1 + \mathbf{g}(M_2 l_2 \sin(\theta_1 + \theta_2)) \\ \mathbf{g} M_2 l_2 \sin(\theta_1 + \theta_2) \end{bmatrix}$$

$$\boldsymbol{\Gamma} = \begin{bmatrix} \boldsymbol{\Gamma}_{1 \text{ actuator}} - \boldsymbol{\Gamma}_{1 \text{ friction}} \\ \boldsymbol{\Gamma}_{2 \text{ actuator}} - \boldsymbol{\Gamma}_{2 \text{ friction}} \end{bmatrix}$$

To check the equation derived above, we simply give the robot arm some initial conditions and add a constant friction in both joints to check whether the total energy decreases all the way down. The ideal friction force $\boldsymbol{\Gamma}_{\text{friction}}$ between each joint in matrix form is

$$\boldsymbol{\Gamma}_{\text{friction}} = \begin{bmatrix} a & b \\ -b & 0 \end{bmatrix} \begin{bmatrix} \dot{\theta}_1 \\ \dot{\theta}_2 \end{bmatrix}$$

The results are shown in figure 11 . The total energy goes down all the way to the equilibrium point. The 1st and 2nd link go to the zero point after a period of time.

VITA

Wei-guang Chen

Candidate for the Degree of

Master of Science

**Thesis: DISCRETE SLIDING MODE CONTROL USING IN A SCARA ROBOT
BY DIGITAL COMPUTER**

Major Field: Mechanical Engineering

Biographical:

**Personal Data: Born in Hwa-lian, Taiwan, December 12, 1965, the son of
Mr. H. K. Chen and Mrs. I. H. Twu.**

**Education: Graduate from Tung-shun High School, Taipei, Taiwan, in
June, 1983; Received the Bachelor of Science degree from Chung Yuan
Christian University in June, 1987; completed requirements for the Master
of Science degree at Oklahoma State University in May, 1993**

**Professional Experience: Squad Leader, Chinese Army, September, 1987, to
July, 1989; Research Assistant, Institute of Nuclear Science, August, 1989,
to June, 1990; Research Assistant, Oklahoma State University, January,
1991, to December, 1991.**